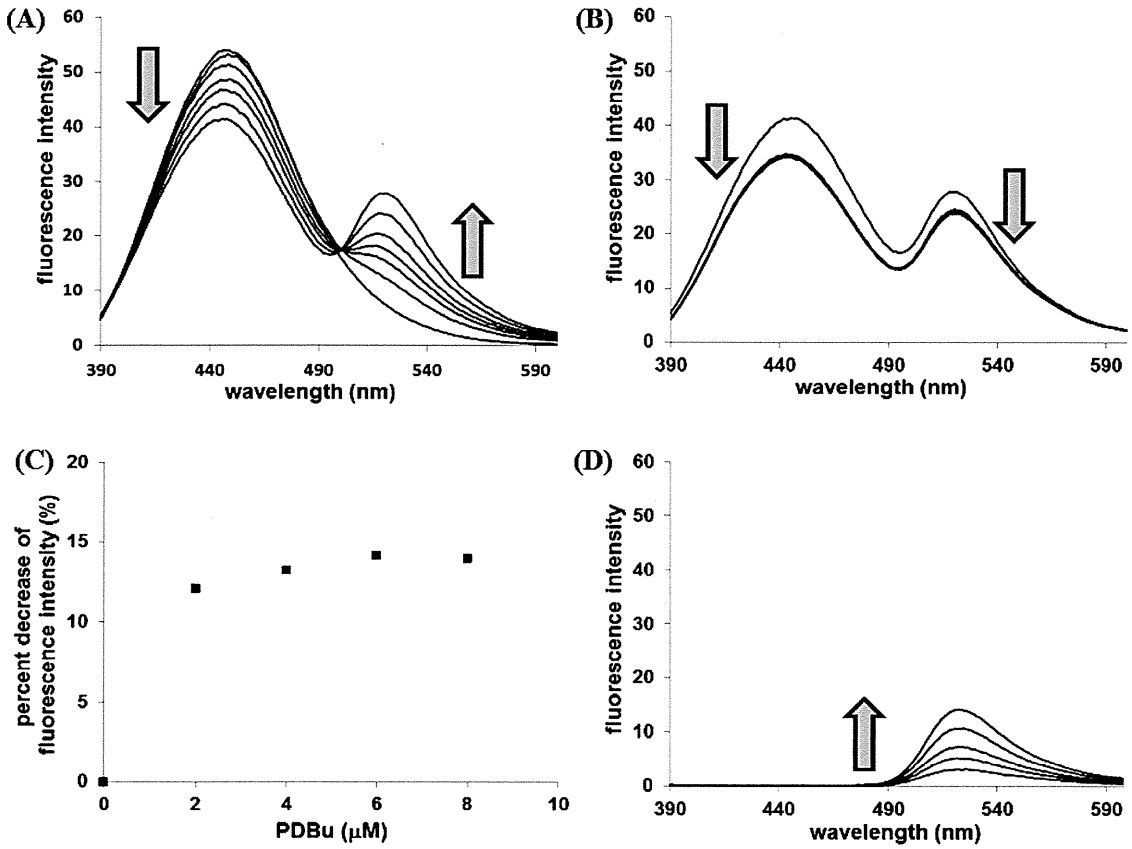

Fig. 3. Changes of Fluorescent Spectra during Titration Experiments

(A) The titration of the acceptor molecule against 200 nM donor molecule. The concentration of the acceptor molecule was increased to 1120 nM (5.6 eq to the donor molecules) by titration. (B) The titration of PDBu against the assay solution containing 200 nM donor molecule and 1120 nM acceptor molecule. The concentration of PDBu was increased to 8 μM (40 eq to the donor molecule) by titration. (C) The plots of percent decrease of fluorescence intensity *versus* the concentration of PDBu at 522 nm. (D) The fluorescent spectra of acceptor molecules (133, 267, 533, 800, 1067 nM). The fluorescence intensity was increased with increasing concentration. The excitation wavelength was 380 nm.

pressure, followed by purification by silica gel column chromatography ($CHCl_3$/MeOH=20 : 1) to give the decanoate **6** (*E* isomer, racemic, 14.7 mg, 28% yield) as an orange oil: *Rf* 0.16 ($CHCl_3$/MeOH=3 : 1); ^{1}H-NMR (400 MHz, $CDCl_3$) δ: 7.30 (1H, d, J=9.2 Hz), 7.02 (1H, s,), 6.57–6.54 (1H, m), 6.51 (1H, d, J=2.8 Hz), 5.97 (1H, s), 4.36–4.26 (2H, m), 3.77–3.75 (2H, m), 3.67 (2H, s), 3.41 (4H, dd, J=6.8, 7.2 Hz), 2.28–2.23 (2H, m), 2.07–2.03 (1H, m), 1.26–1.19 (20H, m), 0.88 (3H, t, J=6.8 Hz). ^{13}C-NMR (125 MHz, $CDCl_3$) δ: 173.40, 171.55, 161.85, 156.45, 151.60, 150.80, 149.13, 133.02, 125.31, 108.80, 108.71, 107.22, 97.74, 87.80, 63.45, 62.87, 44.73, 33.82, 31.83, 29.37, 29.23, 27.63, 24.76, 22.64, 14.09, 12.41. ESI-MS *m/z*: 528.2952 (Calcd for $C_{30}H_{42}O_7N$ $[M+H]^+$: 528.2961).

2-(6-Hydroxy-3-oxo-3*H*-xanthen-9-yl)-5(6)-(prop-2-yn-1-ylcarbamoyl)benzoic Acid[30] 1-Hydroxybenzotriazole monohydrate (HOBt·H_2O) (150 mg, 1.1 mmol), Et_3N (153 mL, 1.1 mmol) were added to a solution of propargylamine hydrochloride (100 mg, 1.1 mmol) in CH_2Cl_2 (10 mL), 5(6)-carboxyfluorescein (376 mg, 1.0 mmol) and 1-ethyl-(3-(3-dimethylamino)propyl)carbodiimide hydrochloride (EDCI) (210 mg, 1.1 mmol) at −8°C, and the resulting mixture was stirred at 0°C for 1 h, and then at room temperature for 2 h. The reaction was quenched with H_2O. The aqueous layer was extracted three times with EtOAc. The combined organic layer was washed with brine, dried over $MgSO_4$, filtrated and concentrated under reduced pressure to afford the crude alkyne. Purification by HPLC (27–36% MeCN/H_2O, 50 min) gave alkynyl fluorescein (mixture of 5-, 6-isomers) (120 mg, 29%) as an orange powder. ESI-MS *m/z*: 414.0997 (Calcd for $C_{24}H_{16}NO_6$ $[M+H]^+$: 414.0978).

Preparation of Fmoc-His(Trt)-Trt(2-Cl)-Resin 2-Chlorotrityl chloride resin (1.2 mmol/g, 1.0 g) (Novabiochem) was treated with Fmoc-His(Trt)-OH (0.4 mmol, 245 mg) and DIPEA (1.6 mmol, 280 μL) in dry *N*,*N*-dimethylformamide (DMF) (6 mL) for 1 h. After washing with dry DMF, CH_2Cl_2, and Et_2O, the resin was dried in a vacuum desiccator. The loading was determined by measuring UV absorption at 301 nm of the piperidine-treated Fmoc-His(Trt)-Trt(2-Cl)-resin (0.26 mmol/g).

Peptide Synthesis All peptides were synthesized by Fmoc-based solid-phase peptide synthesis (SPPS). The following amino acid side-chain protecting groups were used; Boc for Lys, Pbf for Arg, O^{t}Bu for Asp and Glu, Trt for Asn, Cys, and His, ^{t}Bu for Ser, Thr, and Tyr. The coupling reactions were performed by shaking for 1.5–2 h a coupling reaction mixture contained Fmoc-protected amino acid and *N*,*N*′-diisopropylcarbodiimide (DIPCI)/HOBt·H_2O or *O*-benzotriazole-*N*,*N*,*N*′,*N*′-tetramethyluronium hexafluorophosphate (HBTU)/DIPEA/HOBt·H_2O. A solution of 20% piperidine in DMF was used for deprotection of Fmoc groups, achieved by shaking the reaction mixture for 20 min. The δC1b(247–281) fragment was manually constructed on a TGR resin (0.22 mmol/g, 0.68 g). Deprotection and cleavage from the resin was performed by treatment with TFA (10 mL),

m-cresol (0.25 mL), thioanisole (0.75 mL), 1,2-ethanedithiol (0.75 mL), H_2O (0.25 mL), and TIS (0.10 mL). Purification by isocratic RP-HPLC (30% isocratic of MeCN containing 0.1% TFA, *vs.* H_2O containing 0.1% TFA) gave 120 mg (21% yield) of the δC1b(247–281) fragment **11** as a white powder: ESI-MS *m/z*: Found 3828.3 (Calcd for $C_{161}H_{268}N_{51}O_{45}S_6$ $[M+H]^+$: 3828.8). Retention time: 12.3 min with MeCN (30% isocratic).

The δC1b(231–246) and δC1b(231–246)V235Nle(ε-azide) fragment was constructed on an Fmoc-His(Trt)-2-chlorotrithyl resin 0.13 mmol scale using Fmoc-Nle(ε-azide)-OH.[31] Cleavage from the resin was performed by stirring for 2 h with TFE/AcOH/CH_2Cl_2 (1 : 1 : 3, v/v). The resulting protected peptide and HOBt·H_2O (10 eq) were dissolved in DMF, and ethyl 3-mercaptopropionate (20 eq) was added. The mixture was cooled to 0°C, and EDCI (10 eq) was added. The mixture was stirred for 5 h then allowed to reach room temperature. DMF was removed by evaporation, and the crude product was washed with H_2O. Deprotection was performed as in the synthesis of δC1b(247–281) without the addition of EDT. Preparative RP-HPLC (31% isocratic of MeCN) gave 8.8 mg (7% yield) of the δC1b(231–246)V235Nle(ε-azide) thioester **8** as a white powder: ESI-MS *m/z*: Found 2259.1 (Calcd for $C_{101}H_{141}N_{28}O_{26}S_3$ $[M+H]^+$: 2258.1). Retention time: 9.2 min with MeCN (27% isocratic).

Fluorescein Labeling by Click Reaction To a solution of δC1b(231–246)V235Nle(ε-azide) (3 mg, 1.1 μmol) in DMF (120 μL) and H_2O (120 μL) was added 0.2 mM fluorescein alkyne in MeCN/H_2O 1 : 1 (55 μL, 1.1 μmol). After the addition of 0.1 mM $CuSO_4$ in H_2O (130 μL, 13 μmol) and 0.1 mM sodium ascorbate in H_2O (130 μL, 13 μmol), followed by degassing, the reaction mixture was stirred under an Ar atmosphere for 2 h at room temperature. Purification by RP-HPLC (gradient; 26–36% of MeCN, 60 min) gave 1.6 mg (53% yield) of the δC1b(231–246)V235Nle(ε-Fl) (Fl-δC1b(231–281)) thioester **9** as a yellow powder. ESI-MS *m/z*: Found 2671.1 (Calcd for $C_{125}H_{156}N_{29}O_{32}S_3$ $[M+H]^+$: 2671.1). Retention time: 14.2 min with MeCN (26–36%, 30 min).

Condensation of Peptide Fragments by Native Chemical Ligation The δC1b(231–246)V235Nle(ε-Fl) containing the peptide thioester **9** (1.8 mg, 0.66 μmol) and δC1b(247–281) (2.8 mg, 0.60 μmol) were dissolved in 230 μL of 0.1 M phosphate buffer (pH 7.7) containing 6.0 M guanidine hydrochloride (Gn·HCl), 2.0 mM ethylenediaminetetraacetic acid (EDTA), TCEP·HCl (0.95 mg, 3.3 μmol) and 4-mercaptophenylacetic acid (MPAA) (1.4 mg, 8.3 μmol). The reaction mixture was adjusted to approximately pH 7.8 with 8 M NaOH in H_2O. The ligation reaction was performed at 37°C for 5 h under an Ar atmosphere. Purification by RP-HPLC (gradient; 33–38% of MeCN, 60 min) gave 0.54 mg (13% yield) of δC1b(231–281)V235Nle(ε-Fl) (Fl-δC1b(231–281)) **12** as a yellow powder. ESI-MS *m/z*: Found 6365.0 (Calcd for $C_{281}H_{413}N_{80}O_{75}S_8$ $[M+H]^+$: 6363.9). Retention time: 19.0 min with MeCN (33–38%, 30 min).

Degeneration of Peptides A buffer (pH 7.4) containing 6 M Gn·HCl and 50 mM Tris·HCl, dithiothreitol (DTT) was made up to 50 mM, and then the peptide was dissolved in the solution at a concentration of approximately 30 μM. The peptide solution was incubated for 15 min at 30–37°C. The treated peptide solution was dialyzed against 50 mM Tris·HCl (pH 7.4) containing 150 mM NaCl, 1 mM DTT and 0.1 mM $ZnCl_2$ using a Slide-A-Lyzer Dialysis Cassette 3500 MWCO (Thermo Scientific) at 4°C. The dialysis buffer was changed three times. After dialysis the peptide solution was centrifuged at 15000 rpm for 15 min at 4°C, followed by the determination of concentration by UV absorption at 280 nm (ε: Tyr; 1280, Trp; 5690) or at 490 nm (ε: fluorescein; 76900).[32,33]

[^{3}H]PDBu Binding Assay The dissociation constant (K_d) of synthetic δC1b for [^{3}H]PDBu binding and the inhibition constant (K_i) of fluorescent-labeled DAG-lactone for binding of the δC1b domain were assessed by the poly(ethylene glycol) precipitation assay as described previously.[18,27,28]

FRET Experiment A phosphatidylserine (PS) solution (500 μg/mL) was prepared as described below: 50 μL of 10 mg/mL PS in $CHCl_3$ was transferred to a 2 mL micro tube and dried under a stream of N_2 gas. One milliliter of 50 mM Tris·HCl (pH 7.4) was added to the residue and the mixture was sonicated with a probe-type sonicator (5 s bursts ×3). The FRET assay solution (1 mL) containing 200 nM FRET donor molecule, 100 μg/mL PS, and 50 mM Tris·HCl (pH 7.4) was prepared with 200 μL of 0.5 mg/mL PS solution, 2 μL of 100 μM FRET donor stock in dimethyl sulfoxide (DMSO) and 800 μL of 50 mM Tris·HCl (pH 7.4). After addition of 13 μL of 10.5 μM FRET acceptor solution, the assay solution was mixed by pipetting followed by 5 min incubation in the dark. The fluorescent spectra were measured by excitation at 380 nm. The concentration of the FRET acceptor started at 140 nM and increased to 1120 nM. The FRET competitive assay was demonstrated using PDBu as a positive ligand. The competitive assay solution contains 200 nM FRET donor, 1120 nM FRET acceptor, 100 μg/mL PS, and 50 mM Tris·HCl (pH 7.4). The concentration of PDBu started at 2 μM and increased to 8 μM.

Acknowledgments This work was supported by JSPS Core-to-Core Program, A. Advanced Research Networks, and Grants from Takeda Science Foundation.

References

1) Stryer L., Haugland R. P., *Proc. Natl. Acad. Sci. U.S.A.*, **58**, 719–726 (1967).
2) Stryer L., *J. Biochem.*, **287**, 15164–15173 (2012).
3) Antal C. E., Violin J. D., Kunkel M. T., Skovsø S., Newton A. C., *Chem. Biol.*, **21**, 459–469 (2014).
4) Kumar S., Kellish P., Robinson W. E. Jr., Wang D., Appella D. H., Arya D. P., *Biochemistry*, **51**, 2331–2347 (2012).
5) Zwier J. M., Roux T., Cottet M., Durroux T., Douzon S., Bdioui S., Gregor N., Bourrier E., Oueslati N., Nicolas L., Tinel N., Boisseau C., Yverneau P., Charrier-Savournin F., Fink M., Trinquet E., *J. Biomol. Screen.*, **15**, 1248–1259 (2010).
6) Nomura W., Tanabe Y., Tsutsumi H., Tanaka T., Ohba K., Yamamoto N., Tamamura H., *Bioconjug. Chem.*, **19**, 1917–1920 (2008).
7) Nomura W., Ohashi N., Okuda Y., Narumi T., Ikura T., Ito N., Tamamura H., *Bioconjug. Chem.*, **22**, 923–930 (2011).
8) Nishizuka Y., *Science*, **258**, 607–614 (1992).
9) Watanabe T., Ono Y., Taniyama Y., Hazama K., Igarashi K., Ogita K., Kikkawa U., Nishizuka Y., *Proc. Natl. Acad. Sci. U.S.A.*, **89**, 10159–10163 (1992).
10) Mischak H., Pierce J. H., Goodnight J., Kazanietz M. G., Blumberg P. M., Mushinski J. F., *J. Biol. Chem.*, **268**, 20110–20115 (1993).
11) Ghayur T., Hugunin M., Talanian R. V., Ratnofsky S., Quinlan C., Emoto Y., Pandey P., Datta R., Huang Y., Kharbanda S., Allen H., Kamen R., Wong W., Kufe D., *J. Exp. Med.*, **184**, 2399–2404 (1996).
12) Humphries M. J., Limesand K. H., Schneider J. C., Nakayama K. I., Anderson S. M., Reyland M. E., *J. Biol. Chem.*, **281**, 9728–9737 (2006).

13) Newton A. C., *Am. J. Physiol. Endocrinol. Metab.*, **298**, E395–E402 (2010).
14) Marquez V. E., Blumberg P. M., *Acc. Chem. Res.*, **36**, 434–443 (2003).
15) Irie K., Yanagita R. C., Nakagawa Y., *Med. Res. Rev.*, **32**, 518–535 (2012).
16) Yanagita R. C., Nakagawa Y., Yamanaka N., Kashiwagi K., Saito N., Irie K., *J. Med. Chem.*, **51**, 46–56 (2008).
17) Baba Y., Ogoshi Y., Hirai G., Yanagisawa T., Nagamatsu K., Mayumi S., Hashimoto Y., Sodeoka M., *Bioorg. Med. Chem. Lett.*, **14**, 2963–2967 (2004).
18) Ohashi N., Nomura W., Narumi T., Lewin N. E., Itotani K., Blumberg P. M., Tamamura H., *Bioconjug. Chem.*, **22**, 82–87 (2011).
19) Braun D. C., Garfield S. H., Blumberg P. M., *J. Biol. Chem.*, **280**, 8164–8171 (2005).
20) Brumbaugh J., Schleifenbaum A., Gasch A., Sattler M., Schultz C., *J. Am. Chem. Soc.*, **128**, 24–25 (2006).
21) Sharma R., Lee J., Wang S., Milne G. W., Lewin N. E., Blumberg P. M., Marquez V. E., *J. Med. Chem.*, **39**, 19–28 (1996).
22) Furuta T., Takeuchi H., Isozaki M., Takahashi Y., Kanehara M., Sugimoto M., Watanabe T., Noguchi K., Dore T. M., Kurahashi T., Iwamura M., Tsien R. Y., *ChemBioChem*, **5**, 1119–1128 (2004).
23) Tamamura H., Bienfait B., Nacro K., Lewin N. E., Blumberg P. M., Marquez V. E., *J. Med. Chem.*, **43**, 3209–3217 (2000).
24) Tamamura H., Sigano D. M., Lewin N. E., Blumberg P. M., Marquez V. E., *J. Med. Chem.*, **47**, 644–655 (2004).
25) Tamamura H., Sigano D. M., Lewin N. E., Peach M. L., Nicklaus M. C., Blumberg P. M., Marquez V. E., *J. Med. Chem.*, **47**, 4858–4864 (2004).
26) Ohashi N., Nomura W., Kato M., Narumi T., Lewin N. E., Blumberg P. M., Tamamura H., *J. Pept. Sci.*, **15**, 642–646 (2009).
27) Kazanietz M. G., Areces L. B., Bahador A., Mischak H., Goodnight J., Mushinski J. F., Blumberg P. M., *Mol. Pharmacol.*, **44**, 298–307 (1993).
28) Sharkey N. A., Blumberg P. M., *Cancer Res.*, **45**, 19–24 (1985).
29) El Kazzouli S., Lewin N. E., Blumberg P. M., Marquez V. E., *J. Med. Chem.*, **51**, 5371–5386 (2008).
30) Seo T. S., Li Z., Ruparel H., Ju J., *J. Org. Chem.*, **68**, 609–612 (2003).
31) Byrne C., McEwan P. A., Emsley J., Fischer P. M., Chan W. C., *Chem. Commun.* (Camb.), **47**, 2589–2591 (2011).
32) Edelhoch H., *Biochemistry*, **6**, 1948–1954 (1967).
33) Sjöback R., Nygren J., Kubista M., *Spectrochim. Acta [A]*, **51**, L7–L21 (1995).
34) Nomura W., Narumi T., Ohashi N., Serizawa Y., Lewin N. E., Blumberg P. M., Furuta T., Tamamura H., *ChemBioChem*, **12**, 535–539 (2011).

Histochem Cell Biol (2014) 142:473–488
DOI 10.1007/s00418-014-1237-7

ORIGINAL PAPER

Retrograde migration of pectoral girdle muscle precursors depends on CXCR4/SDF-1 signaling

Maryna Masyuk · Aisha Abduelmula · Gabriela Morosan-Puopolo · Veysel Ödemis · Rizwan Rehimi · Nargis Khalida · Faisal Yusuf · Jürgen Engele · Hirokazu Tamamura · Carsten Theiss · Beate Brand-Saberi

Accepted: 5 May 2014 / Published online: 28 June 2014

Abstract In vertebrates, muscles of the pectoral girdle connect the forelimbs with the thorax. During development, the myogenic precursor cells migrate from the somites into the limb buds. Whereas most of the myogenic precursors remain in the limb bud to form the forelimb muscles, several cells migrate back toward the trunk to give rise to the superficial pectoral girdle muscles, such as the large pectoral muscle, the latissimus dorsi and the deltoid. Recently, this developing mode has been referred to as the "In–Out" mechanism. The present study focuses on the mechanisms of the "In–Out" migration during formation of the pectoral girdle muscles. Combining in ovo electroporation, tissue slice-cultures and confocal laser scanning microscopy, we visualize live in detail the retrograde migration of myogenic precursors from the forelimb bud into the trunk region by live imaging. Furthermore, we present for the first time evidence for the involvement of the chemokine receptor CXCR4 and its ligand SDF-1 during these processes. After microsurgical implantations of CXCR4 inhibitor beads in the proximal forelimb region of chicken embryos, we demonstrate with the aid of in situ hybridization and live-cell imaging that CXCR4/SDF-1 signaling is crucial for the retrograde migration of pectoral girdle muscle precursors. Moreover, we analyzed the MyoD expression in CXCR4-mutant mouse embryos and observed a considerable decrease in pectoral girdle musculature. We thus demonstrate the importance of the CXCR4/SDF-1 axis for the pectoral girdle muscle formation in avians and mammals.

Keywords Pectoral girdle muscles · CXCR4/SDF-1 · Time-lapse imaging · Secondary trunk muscles · In ovo electroporation

Electronic supplementary material The online version of this article (doi:10.1007/s00418-014-1237-7) contains supplementary material, which is available to authorized users.

M. Masyuk · A. Abduelmula · G. Morosan-Puopolo · R. Rehimi · N. Khalida · F. Yusuf · C. Theiss · B. Brand-Saberi (✉)
Medical Faculty, Department of Anatomy and Molecular Embryology, Ruhr-University Bochum, Universitätsstraße 150, 44801 Bochum, Germany
e-mail: beate.brand-saberi@rub.de

V. Ödemis · J. Engele
Medical Faculty, Institute of Anatomy, University of Leipzig, Liebigstr. 13, 04103 Leipzig, Germany

V. Ödemis
Faculty of Medicine and Health Sciences, Carl von Ossietzky University Oldenburg, Carl-von-Ossietzky-Str. 9-11, 26129 Oldenburg, Germany

H. Tamamura
Department of Medicinal Chemistry, Institute of Biomaterials and Bioengineering, Tokyo Medical and Dental University, Kanda-Surugadai 2-3-10, Chiyoda-ku, Tokyo 101-0062, Japan

C. Theiss
Department of Cytology, Institute of Anatomy, Ruhr-University Bochum, Universitätsstrasse 150, 44801 Bochum, Germany

Introduction

In vertebrates, skeletal muscles of the body develop from the somites. The dorsal epithelial part of the somite, the dermomyotome, yields various derivates, such as skeletal muscles (Huang and Christ 2000; Yusuf and Brand-Saberi

2006), dermis (Mauger 1972a, b; Kalcheim et al. 1999; Olivera-Martinez et al. 2000, 2002, 2004; Ben-Yair et al. 2003; Ben-Yair and Kalcheim 2005), smooth muscles (Ben-Yair and Kalcheim 2008) and angiogenic cells (Wilting et al. 1995, 2000, 2001). In terms of anatomical localization, the dermomyotome can be divided into a dorsomedial and a ventrolateral portion. The dorsomedial dermomyotome gives rise to the intrinsic back muscles or epaxial muscles, whereas the ventrolateral lip of the dermomyotome (VLL) is the source of the hypaxial musculature (Christ and Ordahl 1995; Huang and Christ 2000). At the occipital, cervical and limb level, migrating premyogenic progenitors delaminate from the ventrolateral dermomyotomal lip, deepithelize, undertake a long-range migration and generate at their target locations hypaxial muscles of extremities, tongue and diaphragm (Christ and Ordahl 1995; Chevallier et al. 1977; Christ et al. 1977; Ordahl and Le Douarin 1992). Thus, the development of hypaxial limb musculature comprises several phases ranging from generation of premyogenic progenitor cells in the VLL, their delamination, migration, proliferation and subsequent differentiation into muscle fibers. Various genes have been identified to regulate the processes responsible for the formation of hypaxial limb musculature. Pax3 is required for the specification and establishment of a myogenic progenitor pool in the ventrolateral dermomyotome (Franz et al. 1993; Bober et al. 1994; Tajbakhsh et al. 1997). Another paired box transcription factor called Pax7 is expressed in chicken embryos by migrating myogenic precursors during the entire migration process, whereas in mice, muscle precursors start to express Pax7 when they have already entered the limb (Marcelle et al. 1995; Mansouri et al. 1996). The tyrosine kinase receptor c-Met is expressed by progenitor cells, while its ligand scatter factor/hepatocyte growth factor (SF/HGF) is secreted along the migration routes in the limb bud mesenchyme. This receptor-ligand pair is essential for the delamination of migrating progenitor cells from the VLL (Bladt et al. 1995; Brand-Saberi et al. 1996; Dietrich et al. 1999). Finally, at their terminal destinations, the progenitor cells start to express myogenic regulatory factors Myf5, Mrf4, MyoD and myogenin, which determine the myogenic differentiation program (Ott et al. 1991; Pownall and Emerson 1992; Sassoon 1993).

In the forelimbs of higher vertebrates, two portions can be distinguished, namely the portion located distal to the shoulder joint (stylopod, zeugopod and autopod) and the proximal portion (scapula and clavicle), referred to as pectoral girdle. The latter connects the distal forelimb part to the trunk. Whereas the mechanisms of the forelimb muscle development have been subject of many studies and publications, little is known about the development of the proximal pectoral girdle muscles. Most recently, Valasek and colleagues reported that superficial pectoral girdle muscles arise from subpopulations of forelimb muscle precursors, which initially migrate into the limb bud and return to the trunk thereafter. This mechanism is referred to as the "In–Out" mechanism and the pectoral girdle muscles are therefore secondary trunk muscles (Valasek et al. 2011; Yusuf and Brand-Saberi 2012). Characteristic superficial pectoral girdle muscles are the large pectoral muscle located ventrally and the latissimus dorsi and the deltoid muscles located dorsally.

Until now, the underlying molecular mechanisms governing the retrograde migration of pectoral girdle myogenic precursors have been insufficiently studied. One potential molecular signal playing a role in the retrograde migration of pectoral girdle muscle precursors is the CXCR4/SDF-1 axis. The chemokine receptor CXCR4 and its only ligand SDF-1 are known to be involved in numerous physiological and pathological processes including hematopoiesis (Bleul et al. 1996), neurogenesis (Lazarini et al. 2003, Pujol et al. 2005), metastasis of cancer cells (Müller et al. 2001; Balkwill 2004; Hiratsuka et al. 2011) and HIV pathogenesis (Deng et al. 1996; Doranz et al. 1996; Feng et al. 1996). Moreover, it has been demonstrated that these molecules are implicated in several migration events during embryogenesis, such as migration of primordial germ cells in zebrafish, avians and mammals (Doitsidou et al. 2002; Knaut et al. 2003; Stebler et al. 2004). Beside this, our and other groups have previously shown that CXCR4 and SDF-1 are required for the migration of myogenic progenitors within the limb bud mesenchyme of developing chicken embryos. Hereby, SDF-1 is expressed by the limb mesenchyme and its gene product serves as a guidance cue for CXCR4 expressing myogenic precursor cells (Vasyutina et al. 2005; Yusuf and Brand-Saberi 2006).

By using sophisticated transplantation techniques, Valasek and coauthors convincingly provide evidence that the superficial pectoral girdle muscles develop from precursor cells initially residing in the forelimb. Based on this finding, they postulate the "In–Out" mechanism as the developing mode for this muscle group. Furthermore, they show the significance of one molecular player, Tbx5, not only for the development of the forelimb, but also for the pectoral girdle musculature in chicken and zebrafish (Valasek et al. 2011). However, until now, the molecular signals involved in this migration of pectoral girdle muscle precursors during the "In–Out" developing mode have not been elucidated. Thus, the purpose of the present study was to further investigate the mechanism of the pectoral girdle muscle formation and the role of the CXCR4/SDF-1 axis during this process. Most recently, by combining in ovo electroporation and tissue slice-cultures with the state-of-the-art imaging techniques of confocal laser scanning microscopy and spinning disc confocal microscopy, our group has been able to visualize by live imaging the migration

of myogenic precursors from the somite into the developing limb bud. Thus, in this technical work, we developed a novel approach for dynamical analysis of cell migration in embryonic tissues (Masyuk et al. 2014). Here, we demonstrate live in detail the migration pattern of the pectoral girdle myogenic precursors and, thus, verify the "In–Out" mechanism consisting of migration into the developing forelimb bud, followed by the retrograde migration in the shoulder region with aid of time-lapse imaging. But most importantly, we show the role of CXCR4 and SDF-1 in the development of pectoral girdle musculature by modifying this signaling during embryonic development of chicken and mice. To this purpose, we blocked the CXCR4/SDF-1 signaling by a specific CXCR4 inhibitor in the shoulder region of chicken embryos and show that the migration of myogenic precursors toward the trunk is affected. Furthermore, our analysis of CXCR4-mutant mice demonstrates considerable decrease of pectoral girdle muscle. Hence, in the present study, we provide for the first time evidence that the CXCR4/SDF-1 axis is crucial for the retrograde migration during formation of pectoral girdle musculature in both avians and mammals.

Materials and methods

In ovo electroporation

Fertilized Lohmann Brown chicken eggs (Gallus domesticus) obtained from a local breeder were incubated at 37.5 °C and 80 % relative humidity until the stages HH14–15 (Hamburger and Hamilton 1951) were reached. To lower the embryo, 2–3 ml of albumen was withdrawn with a sterile syringe at the blunt end. An oval window about 2 cm in length was cut on the upper side of the egg. For a better visualization of the embryo, black drawing ink diluted 1:10 with Locke's solution containing penicillin G (Penicillin G sodium salt, PENNA, Sigma) was injected into the yolk under the blastoderm. The vitelline membrane and the amnion overlaying the embryo were carefully removed with a tungsten needle. The Tol2-EGFP vector system (Koga et al. 1996; Kawakami 2007; Kawakami et al. 2000; Sato et al. 2007) kindly provided as a gift from Koichi Kawakami (Division of Molecular and Developmental Biology, National Institute of Genetics, Mishima, Shizuoka 411-8540, Japan) was mixed with transposase. The Tol2 construct inserted into cells together with transposase enables the electroporated EGFP gene to be stably integrated into chicken chromosomes and allows, thus, a stable expression until embryonic day 12 in somite-derived cells (Sato et al. 2007). As reported before, few crystals of Fast Green FCF (F 7258, Sigma-Aldrich) were added to the plasmid solution to detect the injection (Krull 2004). In total, 2 µl of the DNA solution was aspired in a borosilicate glass capillary attached to a rubber aspirator tube and injected into the somites 16–21 by mouth. To ensure conductivity during electroporation, some drops of Locke's solution were added to the newly injected area. The negative electrode was placed left and the positive electrode right of the embryo and five square pulses of 27.5 V, 20 ms pulse-width at 200 ms intervals between the pulses were applied with the aid of the TSS20 Ovodyne electroporator (Intracel, UK). The negatively charged DNA, thus, moved in the electric field toward the somitic cells adjacent to the anode. The eggs were sealed with medical tape and reincubated until the required stages were reached. The EGFP expression in transfected embryos was visualized with the aid of a fluorescence stereo microscope (M 165 FC, Leica, Germany). The oldest stage used in this study was HH30. All embryos were killed at the end of the study by opening the shell and tearing the allantois and amnion with forceps. No permits were required for the described study, which complied with all relevant regulations.

Implantation of CXCR4 inhibitor (TN14003) beads

Specific low molecular weight CXCR4 inhibitor (TN14003) obtained as a gift from Hirokazu Tamamura's group (Institute of Biomaterials and Bioengineering, Tokyo Medical and Dental University, Tokyo 101-0062, Japan) was dissolved in PBS to a concentration of 15 mg/ml. Heparin-coated acrylic beads, approximately 50–80 µm in diameter (H5263, Sigma, Germany), were rinsed in PBS and soaked in the inhibitor solution overnight at 4 °C. Control beads were incubated under the same conditions in PBS. To implant the beads in the dorsal proximal forelimb region of HH23 chicken embryos, eggs were windowed as previously described, and the extraembryonic membranes overlaying the operation side were carefully removed with a tungsten needle. A tunnel in the mesoderm of the dorsal proximal forelimb region was created with a fine tungsten needle. Using a blunt glass needle, the beads were inserted into the tunnel. The operated eggs were sealed with medical tape and reincubated until the stage HH26–27. Finally, the embryos were either sectioned for live imaging or fixed in 4 % paraformaldehyde and used for in situ hybridization.

Preparation of slice cultures

Chicken embryos were electroporated as previously described and reincubated until the stage HH26. To show live the effects of CXCR4 inhibitors on the retrograde migration of pectoral girdle muscle precursors, beads soaked in CXCR4 inhibitor or in PBS for controls were implanted into electroporated embryos as described above and reincubated until the stage HH26. The embryos

were transferred into ice-cold Hank's solution, where the extraembryonic membranes were removed. Thereafter, transverse slices through the limb region of the embryo were prepared using McIlwain™ Tissue Chopper and collected in Hank's solution. Sections were selected under visual control with a binocular microscope, fixed on custom-made glass coverslips (Ø 32 mm, Kindler, Freiburg, Germany) with the aid of plasma (P3266, Sigma, Germany) coagulated with thrombin (605157, Calbiochem) and covered with nutrient medium preheated to 37 °C. Nutrient medium consists of minimal essential medium (MEM, M2279, Sigma-Aldrich, Germany), supplemented with 10 % fetal horse serum (HS, S9135, Biochrom, Germany), 1 % chicken embryonic extract, 0.6 % glucose, 1 % penicillin (A321-42, Biochrom, Germany) and 1 % L-glutamine (G7513, Sigma-Aldrich, Germany).

Live-cell imaging

The migration of the Tol2-EGFP-transfected premyogenic progenitors within the slice culture was studied with the aid of a confocal laser scanning microscope (CLSM, Zeiss LSM 510) equipped with a laser module containing an Ar laser (488 nm) and a HeNe laser (543 nm). For time-lapse imaging, a Rose chamber was utilized, taking the advantage of a closed system and minimal distance between Zeiss 10×-Apochromate lens (Plan-Neofluar, NA 0.3) and the specimen. To maintain the incubation settings at 37 °C and 5 % CO_2 on the microscope stage, a CTI controller 3700 digital, O_2 controller, Tempcontrol 37-2 digital and the Incubator S_{oxygen} together with the heating insert P (Zeiss) are used. To reduce phototoxicity of the cells and photobleaching of the FP-signal, the excitation intensity was reduced to a minimum (488 nm, 2 %; 543 nm, 11 %) and images were taken every 10 min for a period of up to 24 h. The EGFP-positive cells retained apparently normal active motility and proliferation during the monitoring, indicating the cells were viable.

In situ hybridization

Whole mount in situ hybridization was performed as described previously (Nieto et al. 1996). Briefly, chicken and mouse embryos were fixed in 4 % PFA/PBS, treated with proteinase K, refixed and tested for MyoD, Pax7, SDF-1 and CXCR4 expression using species-specific probes. RNA probe for chicken MyoD was a 1,518-bp probe kindly provided by Bruce Peterson. The probe for mouse MyoD was a 1,833-bp probe obtained as a kind gift from Ketan Patel. A 600-bp Pax7 probe, a 425-bp SDF-1 probe and a 693-bp probe specific for chicken was used. The riboprobes were labeled with digoxigenin RNA labeling kit (Roche diagnostics, Germany). The hybridization product was visualized with an antibody against digoxigenin conjugated to alkaline phosphatase. Hybridized samples were photographed using a stereo microscope (M 165 FC, Leica, Germany) equipped with a digital camera (DFC420 C, Leica, Germany). Subsequently, selected chicken embryos were sectioned using a vibratome (VT1000 S, Leica, Germany) at a thickness of 50 µm and embedded in Aquatex® (108562, Merck, Germany). Paraffin or vibratome sections of mouse embryos were carried out.

Immunohistochemistry

For immunohistochemistry, cryosections or slice cultures of electroporated embryos were fixed in 4 % PFA/PBS. The specimens were permeabilized with 1 % Triton-X-100 in PBS for 10 min. Nonspecific-binding sites were blocked with 2 % goat serum (G9023, Sigma-Aldrich) in PBS for 30 min. Afterward, sections were incubated with the primary antibody MF20 (Developmental Studies Hybridoma Bank; cryosections: 1:500 in PBS, slice cultures 1:50 in PBS) overnight at 4 °C, followed by washing in PBS. Visualization of the primary antibody was achieved by incubating the sections with Tetramethyl Rhodamine Iso-Thiocyanate (TRITC, T5393, Sigma, 1:1,000 in PBS) as secondary antibody for at least 2 h. The nuclei were stained using bisBenzimide H 33342 trihydrochloride (Hoechst, B2261, Sigma-Aldrich, 1:100 in PBS). Finally, the samples were intensively washed in PBS and embedded in Fluoromount™ (K024, Biotrend, Germany) mounting medium.

Confocal laser scanning microscopy

Immunoreactivity was analyzed with the aid of a confocal laser scanning microscope (CLSM; LSM 510 Meta, Zeiss, Germany) in combination with Zeiss 40× oil immersion lens (Plan-Neofluar, NA 1.3). To cover the whole extension of the section, z-stack mode was used.

Apoptosis test

Apoptosis test was performed after implantation of TN14003 beads in chicken embryos, using terminal deoxynucleotidyl transferase dUTP nick end labeling (TUNEL) assay (Gavrieli et al. 1992). Paraffin sections of chicken embryos were incubated with 0.5 % pepsin in Aqua, HCl at 39 °C for 15 min. For positive controls, bovine pancreas DNase treatment was performed for 45 min at 39 °C. All sections were quenched of endogenous peroxidase in 3 % hydrogen peroxidase in methanol for 5 min. For TdT labeling, the specimens were first incubated for 10 min in TdT buffer and then in labeling mixture for 90 min at 39 °C. Thereafter, the sections were treated with Streptavidin-HRP

for 1 h at room temperature. For AEC (3-amino-9-ethylcarbazole) reaction, AEC staining kit (AEC101, Sigma, Germany) was used. The slides were incubated with the AEC substrate reagent for 20 min at room temperature.

Results

Lineage tracing of pectoral girdle muscles

To trace the myogenic precursors during formation of superficial pectoral girdle muscles, we electroporated the lateral dermomyotome of the somites 16–21 in HH14–15 chicken embryos using the Tol2-EGFP construct. These somites are adjacent to the forelimb bud and were previously described to give rise to the brachial musculature (Beresford et al. 1978; Beresford 1983). Chicken embryos were reincubated until stage HH30 and observed in ovo at regular intervals (Fig. 1). Initially restricted to the lateral dermomyotome at stage HH18 (Fig. 1a), the Tol2-EGFP-labeled premyogenic progenitor cells were detectable in the developing limb bud at stage HH23 (Fig. 1b). From stage HH26 onwards, muscle blastemas were not limited to the forelimb, but extended to the shoulder region (Fig. 1c, d). Subsequently, at stage HH30, EGFP-positive superficial pectoral girdle muscles were identifiable, on the ventral side the large pectoral muscle and on the dorsal side the latissimus dorsi and deltoid (Fig. 1e, f, $n = 25/28$). Hence, the brachial somites 16–21 do not only give rise to the forelimb muscles, but also to the superficial pectoral girdle muscles.

Live-cell imaging of migratory myogenic progenitors

In order to further examine the migration pattern of myogenic precursor cells, the ventrolateral dermomyotome of HH14–15 chicken embryos was electroporated with the Tol2-EGFP construct as described above and reincubated for certain periods. Slice cultures of the forelimb region of these embryos were captured with the aid of CLSM for approximately 24 h ($n = 15$). This advanced imaging technique allowed us to track precisely the myogenic precursors along their migration pathways. At stage HH23, the migration of the premyogenic cells from the ventrolateral dermomyotome into the forelimb bud was already completed and the myogenic precursors were situated dorsally and ventrally in the limb bud (data not shown). At stage HH26, the EGFP-labeled progenitor cells were no longer restricted to the forelimb, but they were also detectable in the dorsal and ventral trunk region (Fig. 2). Furthermore, with aid of the time-lapse imaging data, an active retrograde migration of individual muscle precursor cells from the forelimb bud toward the pectoral girdle region was clearly visible (Fig. 2; supplement movie 1). Thus, our results demonstrate live the retrograde migration of the pectoral girdle muscle precursors from the forelimb bud to the pectoral girdle region.

Analysis of SDF-1, CXCR4, Pax7 and MyoD expression pattern in the forelimb and pectoral girdle region of chicken embryos

Using in situ hybridization with chicken-specific probes, we analyzed the normal expression pattern of the chemokine receptor CXCR4 and its ligand SDF-1 as well as of Pax7, a gene expressed by migrating myogenic precursors and the myogenic regulatory factor MyoD in the developing forelimb and pectoral girdle region of HH24 and HH26 chicken embryos. At stage HH24, transcripts of SDF-1 are observable in the forelimb bud, whereas at stage HH26, it is additionally expressed in the dorsal pectoral girdle region (Fig. 3a, b). Analogously, expression of its receptor CXCR4 is visible in the forelimb mesenchyme at stage HH24, while at stage HH26, CXCR4-positive cells are also detectable being scattered in and around the pectoral girdle region (Fig. 3c, d). Pax7, a marker of the migrating myogenic precursors, is strongly expressed in the forelimb at both stages, whereby at stage HH26, its expression extends into the proximal forelimb bud (Fig. 3e, f). The expression of the myogenic regulatory factor MyoD is clearly visible in the forelimb bud at both stages. Nevertheless, at stage HH26, the band of MyoD-positive cells is broader than at stage HH24 and is additionally detectable in the dorsal pectoral girdle region (Fig. 3g, h).

Thus, our expression analysis of the myogenic markers Pax7 and MyoD strengthens the hypothesis of the "In–Out" migration during development of pectoral girdle muscles. Furthermore, our results concerning the expression pattern of the chemokine receptor CXCR4 and its ligand SDF-1 suggest a potential involvement of this signaling pathway during the retrograde migration of pectoral girdle muscle precursors.

CXCR4 inhibitor TN14003 affects the retrograde migration of pectoral girdle myogenic precursors in chicken embryos

To investigate the functional significance of the chemokine receptor CXCR4 during the retrograde migration of myogenic pectoral girdle muscle precursors, we implanted acrylic beads soaked in the specific low molecular weight CXCR4 inhibitor TN14003 (Tamamura et al. 1998, 2001) in the dorsal proximal forelimb bud of chicken embryos at stage HH23. Subsequently, at stage HH26, the MyoD expression in the pectoral girdle region was significantly reduced after implantation of CXCR4 inhibitor beads as compared to the control side (Fig. 4a, b, $n = 35/41$). In controls, PBS beads did not show any effect on the

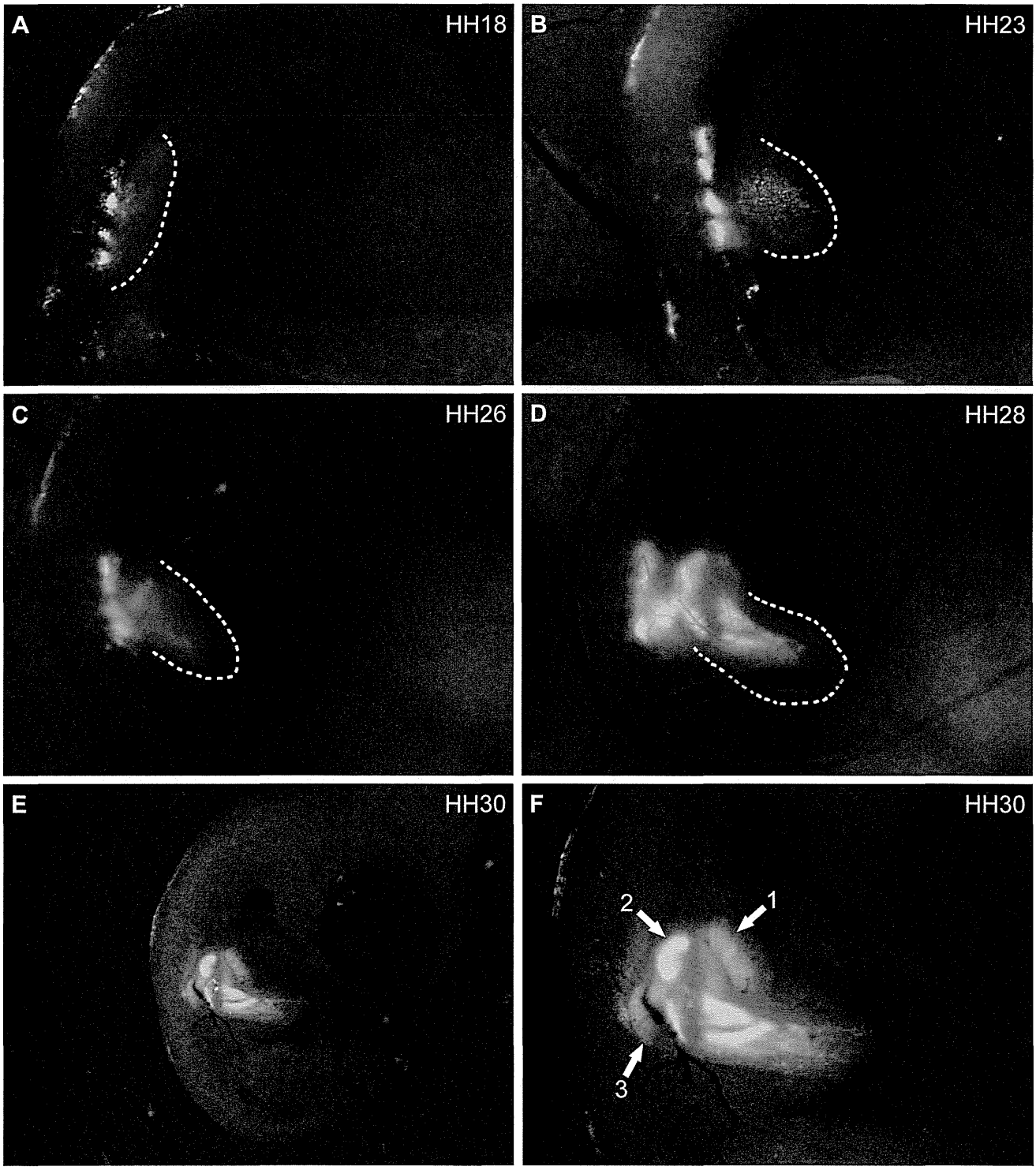

Fig. 1 Somitic origin of the pectoral girdle muscles. The ventrolateral dermomyotomes of the somites 16–21 in HH14 chicken embryo were electroporated using a Tol2-EGFP construct. Embryos were reincubated and observed in ovo using a fluorescence microscope. **a–d** The *dotted line* indicates the developing limb bud. **a** At stage HH18, EGFP-labeled cells were detectable in the ventrolateral dermomyotome and individual cells delaminated and migrated toward the developing limb bud. **b** Numerous premyogenic precursors have already entered the limb bud at stage HH23. **c** At stage HH26, a further increase of the EGFP-positive cells in the limb was observable. **d** Individual muscle blastemas could be distinguished at HH28, but at that time, they were not limited to the forelimb, but extended to the shoulder region. **e**, **f** At stage HH30, EGFP-positive pectoral girdle muscles were identifiable, such as (*1*) the large pectoral muscle, (*2*) the deltoid and (*3*) the latissimus dorsi

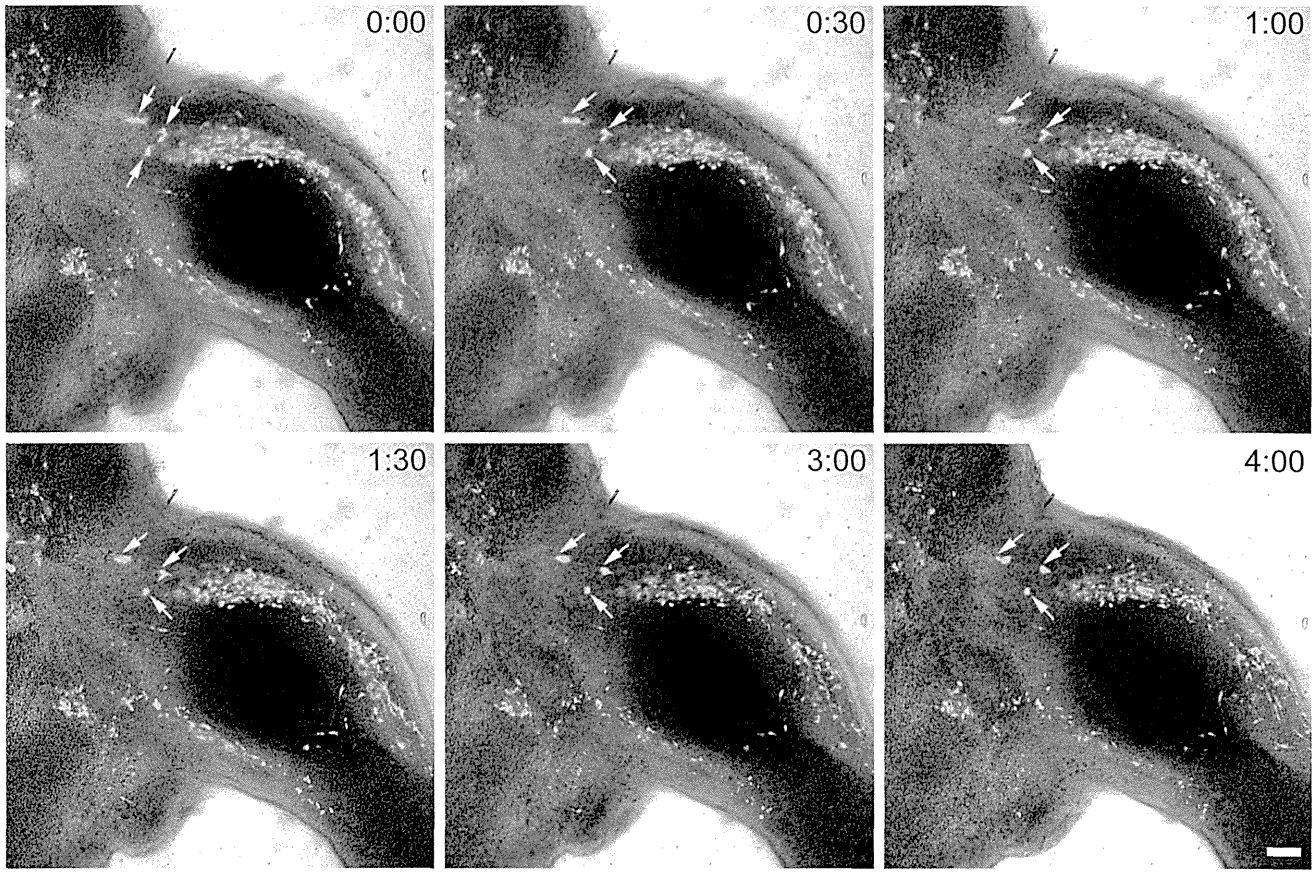

Fig. 2 Time-lapse imaging of the retrograde migration of pectoral girdle muscle precursors. Premyogenic precursor cells were labeled with the Tol2-EGFP construct by electroporation of the ventrolateral dermomyotomes of HH14 chicken embryos. After reincubation up to stage HH26, time-lapse imaging on transverse slice cultures of the forelimb region was performed. The myogenic precursor cells (*green*) were detectable in the dorsal and ventral forelimb bud and trunk region, respectively. Individual cells underwent an active retrograde migration from the forelimb bud toward the thorax (*white arrows*), representing the "Out"-phase of the "In–Out" mechanism required for the pectoral girdle muscle formation. See also Movie 1 in supplementary material. *Scale bar* 100 μm

MyoD expression in the pectoral girdle region (Fig. 4c, d, $n = 45/45$). These results were confirmed by analyzing transverse sections at the forelimb level of these embryos.

Given the fact that the CXCR4/SDF-1 axis is known to be involved in numerous migration processes, these findings suggest that the CXCR4 inhibitor affected the retrograde migration of the pectoral girdle muscle precursor cells. To confirm this hypothesis, we performed time-lapse imaging in slice cultures of chicken embryos. To this purpose, chicken embryos at stage HH14 were electroporated with the Tol2-EGFP construct. After 2 days of reincubation, when the embryos reached stage HH23, beads soaked in CXCR4 inhibitor solution or, for controls, in PBS were implanted into the dorsal proximal forelimb region. After another day of reincubation, time-lapse imaging was performed with slice cultures of these embryos. At stage HH26, the EGFP-labeled myogenic precursor cells were detectable in the dorsal and ventral premuscle mass of the forelimb bud (Figs. 5, 6; supplement movies 2, 3). In our time-lapse imaging analysis in slice cultures of chicken embryos after implantation of CXCR4-inhibitor-soaked beads, we observed highly active movements of EGFP-positive cells which, however, did not succeed to penetrate the TN14003-soaked area in order to reach the pectoral girdle region (Fig. 5; supplement movie 2). By contrast, in slice cultures of chicken embryos after implantation of PBS-soaked control beads, the EGFP-labeled myogenic precursor cells migrated in the retrograde direction toward the trunk passing the acrylic bead with ease (Fig. 6; supplement movie 3).

Taken together, these results show that the CXCR4 inhibitor affects the retrograde migration of myogenic precursor cells required for the formation of pectoral girdle muscles in chicken embryos.

CXCR4 inhibitor TN14003 does not cause cell death

To exclude the possibility that CXCR4 inhibitor affects the retrograde migration of myogenic precursor cells by

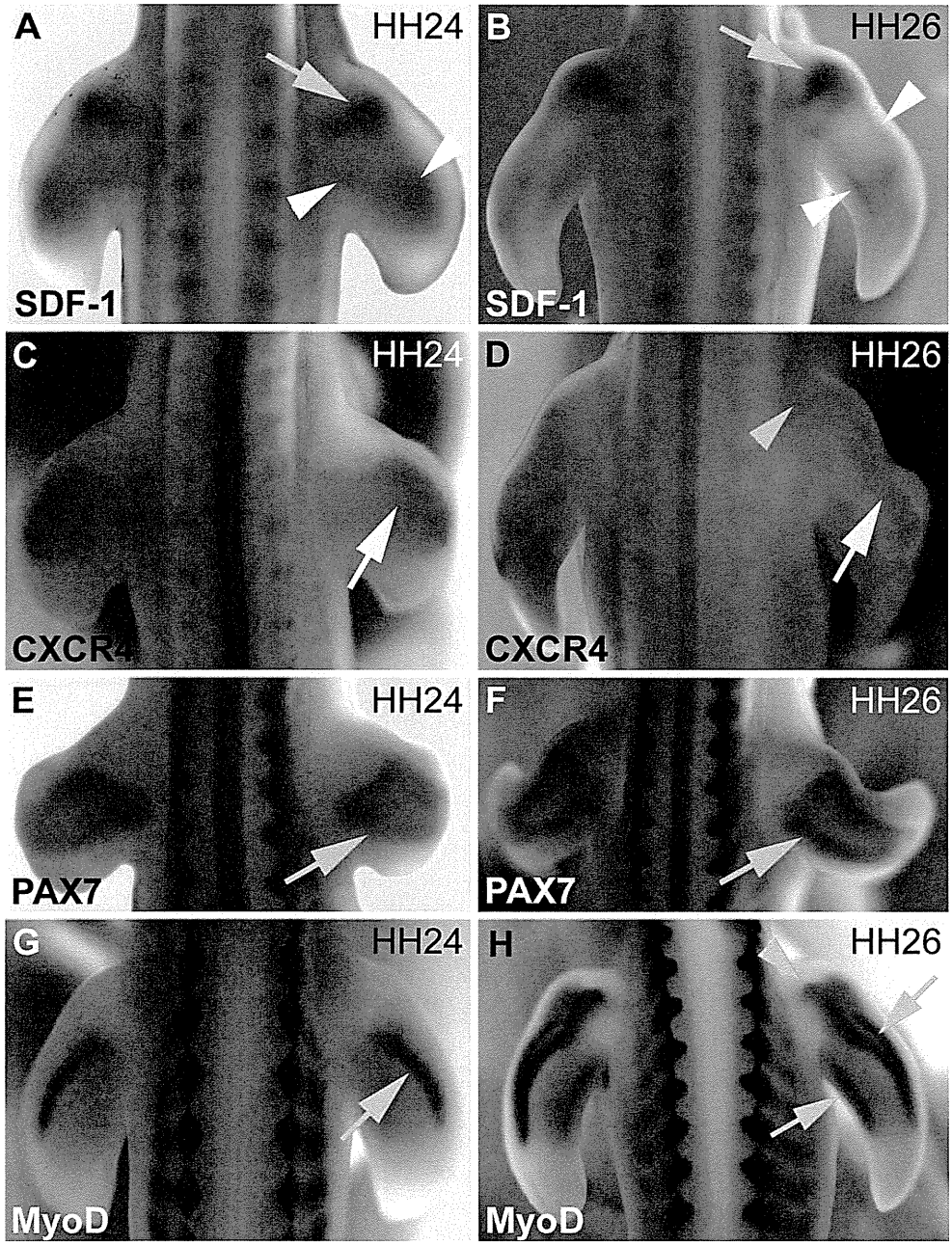

Fig. 3 Expression of SDF-1, CXCR4, Pax7 and MyoD in the pectoral girdle region of chicken embryos. The expression pattern of the stated genes in HH24 and HH26 chicken embryos was analyzed using in situ hybridization. **a**, **b** At stages HH24 and HH26, transcripts of SDF-1 are visible in the dorsal forelimb mesenchyme (*white arrowheads*) as well as in the shoulder region (*green arrows* in **a**, **b**). **c**, **d** At both stages, CXCR4 is prominently expressed in the dorsal forelimb bud (*white arrows*). At stage HH26, few CXCR4-positive cells are observable in and around the pectoral girdle region (*green arrowhead* in **d**). **e**, **f** Strong Pax7 expression is detectable in the dorsal forelimb mesenchyme at stages HH24 and HH26, whereby at stage HH26, Pax7 expression extends into the proximal forelimb (*green arrows* in **e**, **f**). **g**, **h** At stage HH24, MyoD is expressed in the dorsal forelimb bud (*green arrow* in **g**), whereas at stage HH26, the MyoD expression domain is not restricted to the distal forelimb (*green arrows* in **h**), but extends out into the shoulder region (*green arrowhead* in **h**)

inducing cell death, we additionally performed an apoptosis test after implantation of TN14003-soaked beads using the TUNEL assay. Here, no increased apoptosis could be observed in the area around the CXCR4 inhibitor bead (supplement Fig. S1 A,B). To prove the significance of this result, in tissue sections treated with bovine pancreas

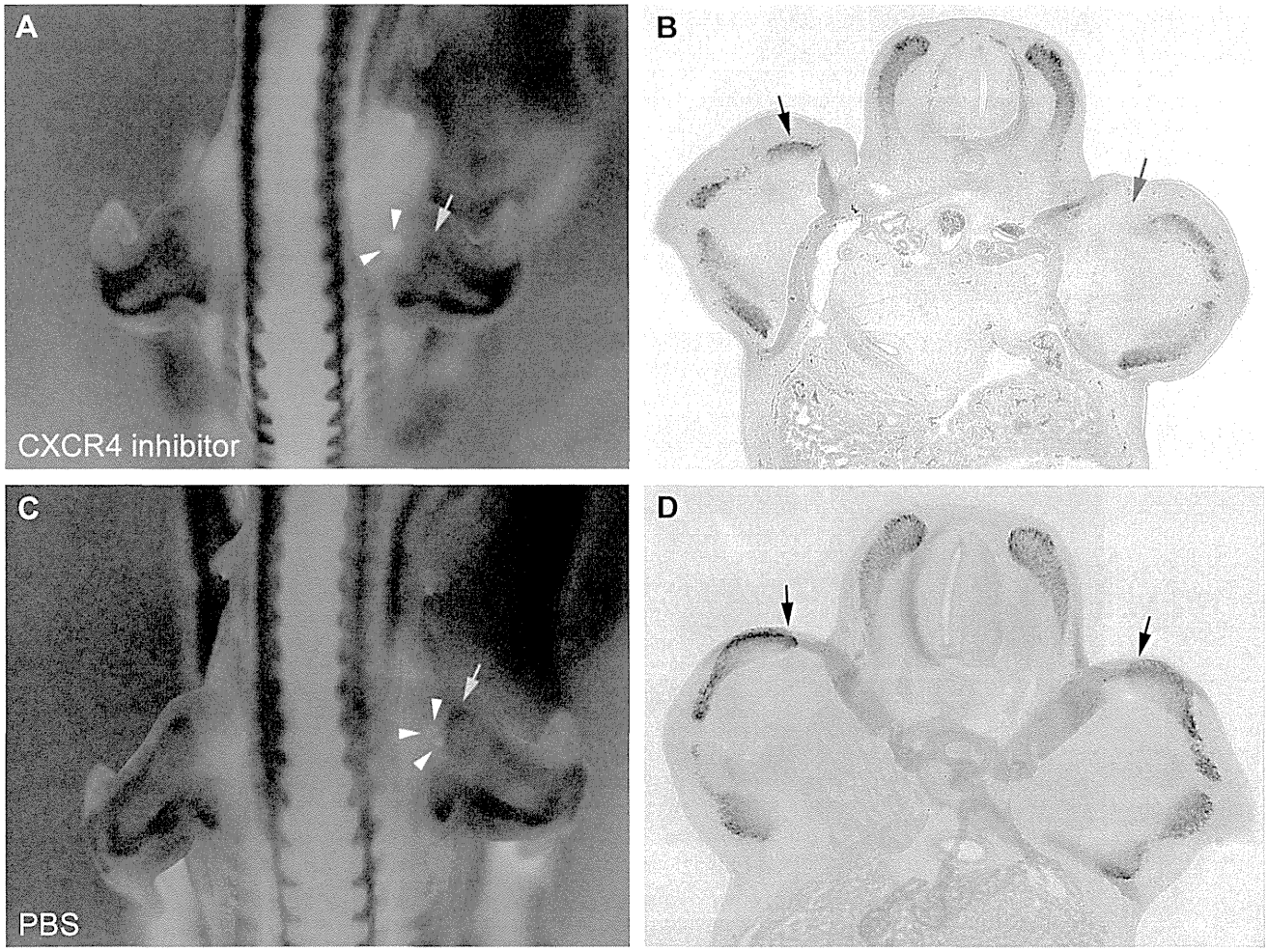

Fig. 4 CXCR4 inhibitor TN14003 affects the formation of pectoral girdle muscle blastemas. Acrylic beads soaked in specific CXCR4 inhibitor TN14003 or PBS, for controls, were implanted into the dorsal proximal forelimb region of HH23 chicken embryos. The embryos were reincubated up to stage HH26 and muscle masses were analyzed using in situ hybridization for MyoD expression. **a**, **b** The MyoD expression in the dorsal shoulder region was considerably reduced (*green arrow* in **a**, *red arrow* in **b**) after implantation of CXCR4 inhibitor beads (*white arrowheads* in **a**) as compared to the control side (*black arrow* in **b**). **c**, **d** PBS beads (*white arrowheads* in **b**) did not show any effect on the MyoD expression in the dorsal pectoral girdle region (*green arrow* in **c**, *black arrows* in **d**). **b**, **d** are transverse sections at forelimb level of the embryos showed in **a**, **c**)

DNase I that cleaves the DNA and was used as positive control, numerous apoptotic cells were detectable in the entire specimen (supplement Fig. S1 C,D).

Tol2-EGFP-transfected cells are not affected by electroporation and develop into muscle cells

Immunohistochemical stainings using MF20, an established marker for muscle cells, demonstrated an overlap of EGFP and MF20 expression (Fig. 7), showing that Tol2-EGFP-labeled cells are myogenic precursor cells and develop into muscle fibers. In slice culture of a Tol2-EGFP-electroporated chicken embryo, we observed contractile and viable EGFP-positive fibers after seven days of reincubation (supplement movie 4). We thus conclude that the electroporation technique does not affect the physiological development of myogenic precursor cells.

Mice deficient in CXCR4 exhibit impaired pectoral girdle muscle formation

Additionally, we examined the development of pectoral girdle muscles in mice carrying a mutation in the CXCR4 gene (Ma et al. 1998; Zou et al. 1998). In situ hybridization using a mouse-specific MyoD probe was used to visualize the muscle blastemas. First, we analyzed the MyoD expression in wildtype mouse embryos ($CXCR4^{+/+}$) and identified individual pectoral girdle muscles, such as the latissimus dorsi, the acromiotrapezius, the spinotrapezius and the spinodeltoid muscle (Fig. 8e, $n = 8/8$).

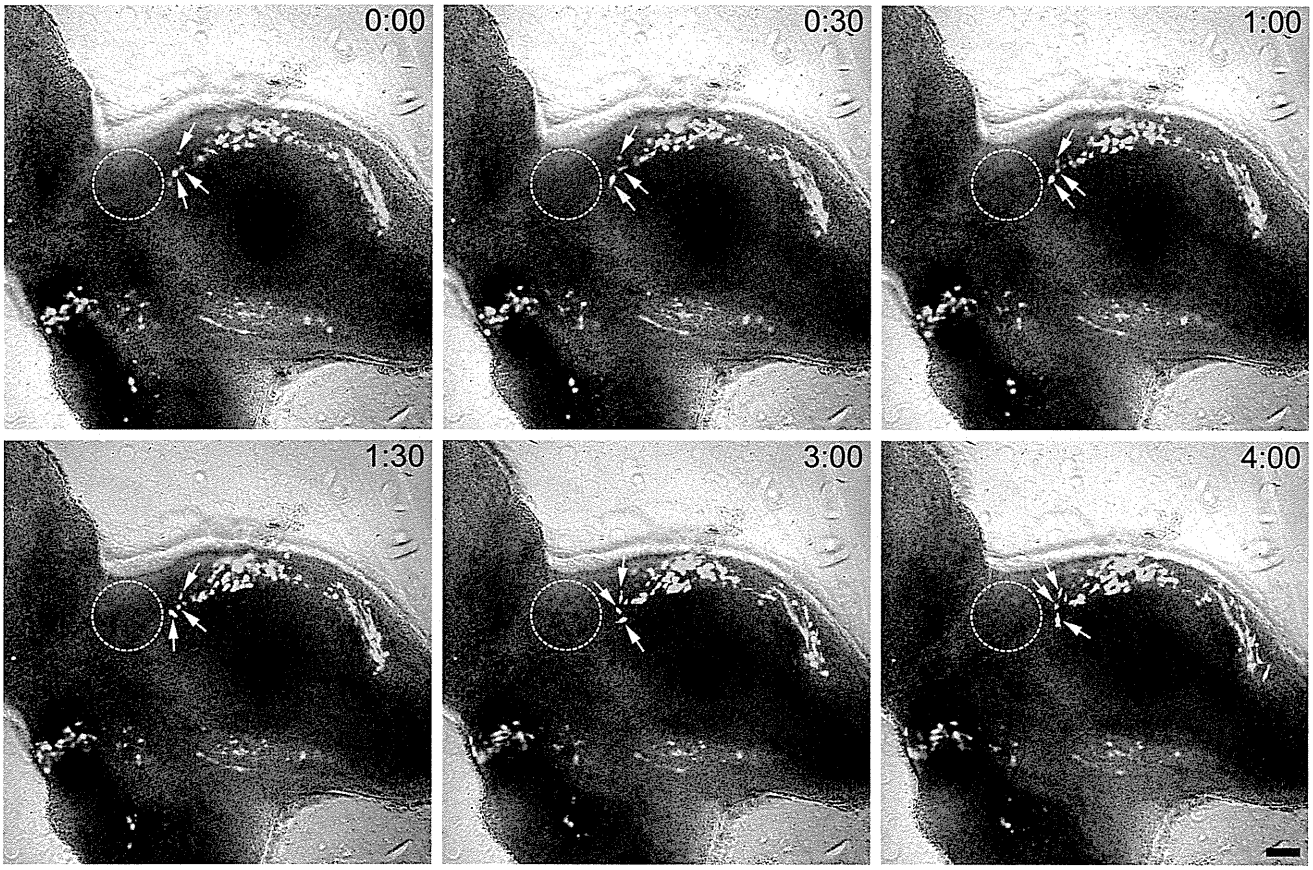

Fig. 5 CXCR4 inhibitor TN14003 affects the retrograde migration of pectoral girdle muscle precursors. Premyogenic precursor cells were labeled with the Tol2-EGFP construct by electroporation of the ventrolateral dermomyotome of HH14 chicken embryos. After reincubation up to stage HH23, acrylic beads soaked in specific CXCR4 inhibitor TN14003 were implanted into the dorsal proximal forelimb region. At stage HH26, time-lapse imaging on transverse slice cultures of the forelimb region was performed. The myogenic precursor cells (*green*) were detectable in the dorsal and ventral forelimb region. The *dotted circle* indicates the area containing the CXCR4 inhibitor solution. The myogenic cells showed highly active movements and proliferation (*white arrows*), but did not succeed in penetrating the CXCR4 inhibitor area and were thus inhibited in their retrograde migration. See also Movie 2 in supplementary material. *Scale bar* 100 μm

In the homozygous ($CXCR4^{-/-}$, $n = 6/6$) E14.5 mouse embryos, we could observe considerably less differentiated pectoral girdle muscle blastemas and, therefore, a decreased MyoD expression in the pectoral girdle region as compared to the wildtype ($CXCR4^{+/+}$) with a strong MyoD expression in all four pectoral girdle muscles stated above (Fig. 8f). In transverse sections at forelimb level of the mouse embryos, we could confirm that the pectoral girdle muscle masses were substantially reduced in the homozygous ($CXCR4^{-/-}$) embryos (Fig. 8b, d) in comparison with the wildtype ($CXCR4^{+/+}$) mice (Fig. 8a, c). In heterozygous littermates, the decrease in pectoral girdle muscles was visible, but less pronounced (not shown). Strikingly, there was no significant difference in MyoD expression in distal forelimb muscles between the homozygous ($CXCR4^{-/-}$) and the wildtype ($CXCR4^{+/+}$) mouse embryos.

Discussion

The results of the present study show that the CXCR4/SDF-1 signaling is required for the pectoral girdle muscle formation in chicken and mice. Moreover, with the aid of time-lapse imaging, we visualized live by time-lapse imaging in detail the effects of CXCR4 inhibitor on the retrograde migration of myogenic precursors from the limb toward the trunk resulting in a failure to undergo retrograde migration in the sense of the well-described "In–Out" mechanism (Valasek et al. 2005, 2011).

Somitic origin of pectoral girdle muscles

More than 30 years ago, Beresford and colleagues performed interspecific chimaera studies by grafting somites from quail to chicken embryos and reported that all

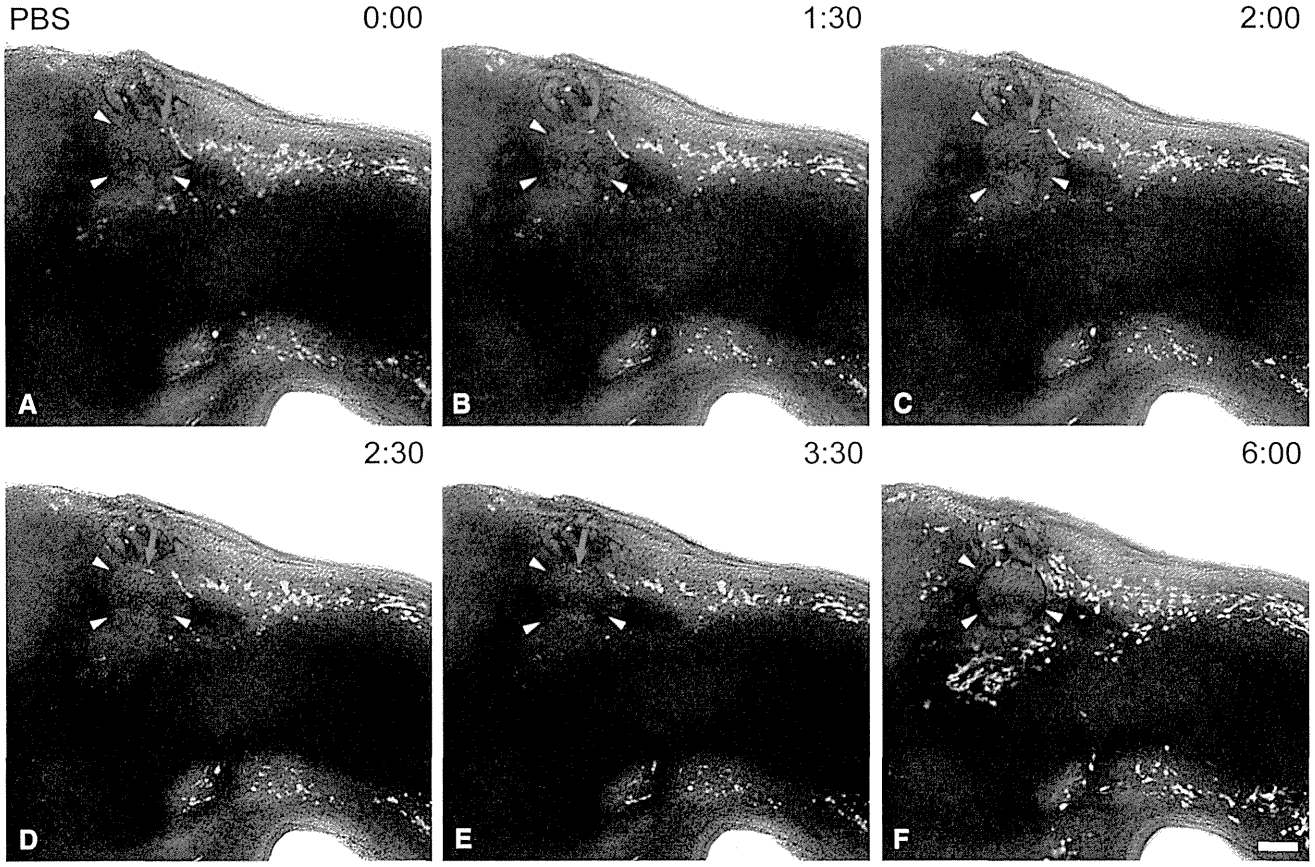

Fig. 6 The acrylic bead does not mechanically interfere with the retrograde migration of pectoral girdle muscle precursors. Premyogenic precursor cells were labeled with the Tol2-EGFP construct by electroporation of the ventrolateral dermomyotome of HH14 chicken embryos. After reincubation up to stage HH23, PBS-soaked acrylic beads were implanted into the dorsal proximal forelimb region. At stage HH26, time-lapse imaging on transverse slice cultures of the forelimb region was performed. **a–e** The myogenic precursor cells (*green*) were detectable in the dorsal and ventral forelimb region. The *white arrowheads* indicate the acrylic control bead soaked in PBS. During the monitoring period, the myogenic cells revealed active motility in the area of the implanted PBS bead. The labeled cell (*red arrow*) actively moved in the retrograde direction toward the trunk passing by the acrylic bead without difficulties. Thus, the retrograde migration of the myogenic cells was not mechanically affected by the bead. **f** The migration route of the myogenic cells is marked by the *dotted red* arrow. See also Movie 3 in supplementary material. *Scale bar* 100 μm

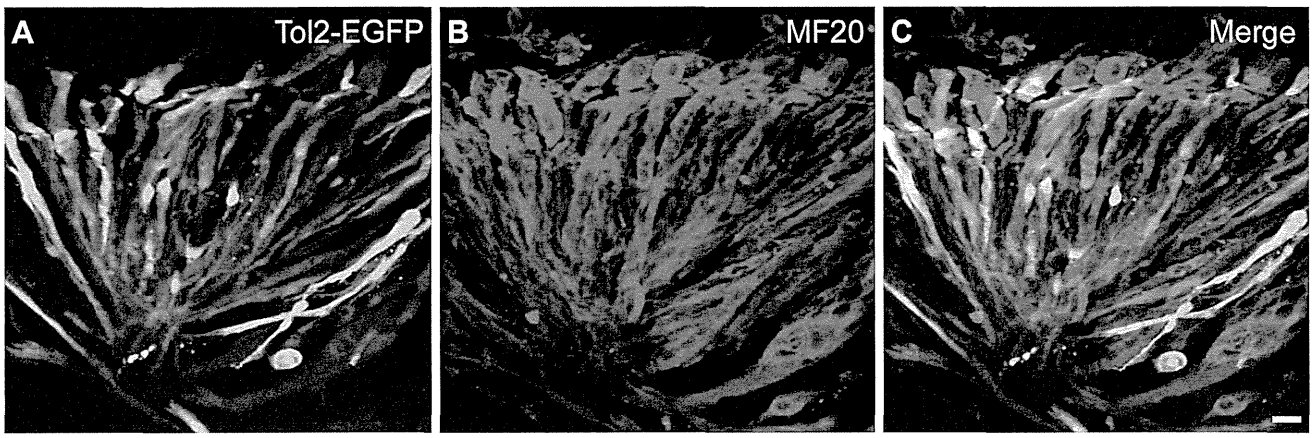

Fig. 7 Tol2-EGFP-transfected cells develop into muscle cells. The ventrolateral dermomyotome of HH14 chicken embryo was transfected with Tol2-EGFP construct using in ovo electroporation. After reincubation, immunohistochemical staining using MF20 as marker for muscle cells was performed and analyzed using CLSM. **a** The Tol2-EGFP-labeled fibers (*green*) also express, **b** MF20 (*red*). **c** In the merged image, the overlap of the Tol2-EGFP and MF20 signal is clearly visible

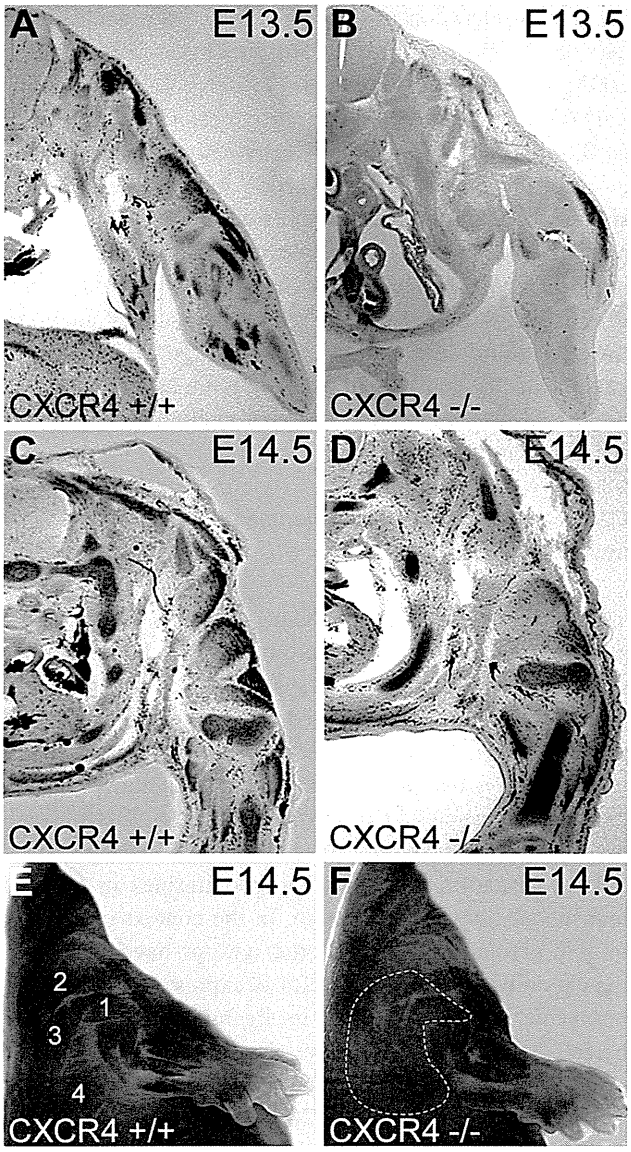

Fig. 8 Mice deficient in CXCR4 exhibits impaired pectoral girdle muscle formation. Muscle development in E13.5 and E14.5 wildtype and CXCR4-mutant mouse embryos was analyzed using in situ hybridization for MyoD. **a–d** In transverse sections through the forelimb region of E13.5 and E14.5 wildtype and CXCR4-mutant mouse embryos, the pectoral girdle muscle blastemas were clearly decreased in the homozygous (**b**, **d**) embryos in comparison to the wildtype mice (**a**, **c**). **e** The normal MyoD expression pattern in E14.5 wildtype mouse embryos is visible. The following pectoral girdle muscles were identifiable: the spinodeltoid muscle (*1*), the acromiotrapezius (*2*), the spinotrapezius (*3*) and the latissimus dorsi (*4*). **f** The muscle blastemas in the pectoral girdle region of the homozygous E14.5 CXCR4-mutant mouse embryo were considerably less developed (*dotted line*) as compared to the wildtype mouse embryo (**e**), which led to a reduced MyoD expression domain in this area. By contrast, the forelimb muscle blastemas of the mutant mouse embryo were clearly visible and unaffected, showing a strong MyoD expression and, thus, did not differ from the one in the forelimbs of wildtype mouse embryos (**e**)

brachial muscles in the avian embryo derive from somites 16–21. This muscle group includes the wing-associated muscles of the shoulder and thorax, and thus, also the deltoid, the pectoral and the latissimus dorsi (Beresford et al. 1978; Beresford 1983). Our study confirmed those findings by using the technique of in ovo electroporation, which allowed us to target the specific somite compartment containing migrating premyogenic progenitors, the ventrolateral dermomyotome. Hence, we could stepwise observe the muscle development in real time in the developing embryo. The EGFP-tagged progenitor cells were detectable in the ventrolateral dermomyotome lip at stage HH18. Moreover, we could observe some cells located outside of the somite, which suggests the delamination of migrating myogenic progenitors from the VLL. After another 24 h of reincubation, at stage HH23, numerous myogenic precursors were detectable in the forelimb bud, which implies that migration had meanwhile proceeded from the VLL into the limb. This is in line with previous studies concerning the limb muscle development (Christ et al. 1977; Ordahl and Le Douarin 1992; Christ and Brand-Saberi 2002). Finally, at stage HH30, apart from forelimb muscles, we also identified EGFP-positive pectoral girdle muscles, namely the deltoid, the pectoral and the latissimus dorsi. This implicates that the pectoral girdle muscle precursors originate from the same axial somitic levels 16–21 that give rise to forelimb muscles.

Migration during formation of pectoral girdle muscles

Several groups have suggested that the pectoral girdle muscles arise from premuscle masses in the developing limb bud by mechanisms of secondary migration out from the limb to the trunk (Beresford et al. 1978; Sullivan 1962; Grim 1971; Lanser and Fallon 1987; Nagashima et al. 2009). Recently, by use of transplantation techniques, Valasek and colleagues could show that the pectoral and latissimus dorsi muscles, which belong to the superficial pectoral girdle muscles, develop from a population of myogenic precursor cells that temporarily reside in the limb. They termed this developing mode the "In–Out" mechanism (Valasek et al. 2011). Our lineage tracing experiments strengthen these results, as after electroporation of brachial somites, myogenic cells were discernible in the limb bud, before they formed pectoral girdle muscle blastemas. Furthermore, our expression analysis of Pax7, a gene expressed by migrating myogenic precursors and the myogenic regulatory MyoD in chicken embryos are also in line with Valasek's results. Additional to our morphological data, the present study visualizes live the migration

pattern of pectoral girdle muscle precursors. In our recent work, by combining the transfection method of in ovo electroporation and the use of tissue slice-cultures with the state-of-the-art imaging technique of confocal laser scanning microscopy, we developed a novel approach to study migrational events in embryonic tissues. The combination of these techniques allowed us to observe migrating premyogenic progenitors which delaminate from the ventrolateral dermomyotome, enter the forelimb bud and migrate to the ventral and dorsal side of the limb (Masyuk et al. 2013). Here, we use this novel technique to visualize the retrograde migration during development of pectoral girdle musculature. We could observe individual somite-derived labeled cells from various locations within the limb moving actively into the opposite direction from the forelimb bud toward the trunk region, which clearly shows the retrograde migration of myogenic precursors. This is required for the formation of secondary trunk muscles. Thus, we could not only verify, but also demonstrate live the "In–Out" mechanisms during formation of pectoral girdle musculature.

Moreover, our time-lapse imaging data allowed us to observe migrating myogenic cells on their pathways to their target locations and analyze their behavior during this process. The observation of numerous cell divisions that occur during this development indicate the high proliferation rate of myogenic precursors during the entire migration period.

The classification of pectoral girdle musculature in deep and superficial muscles proposed by Valasek et al. in the study described before is not only based on their final anatomical position, but also reflects the distinct development modes of these muscle groups. Their grafting experiments in avians showed that, contrary to the superficial pectoral girdle muscles, the deep shoulder girdle muscles, such as rhomboidei or avian serrati, do not deploy the "In–Out" mechanism. They thus assumed that the deep shoulder girdle muscles develop locally from the myotome by myotomal extension (Valasek et al. 2011). Nevertheless, the developing mode of this muscle group has not been visualized in the stated study. Further work is therefore required to demonstrate properly the development of deep pectoral girdle muscles. To this purpose, the same methods as those used in our present study to show the origin and developing mode of the superficial shoulder girdle muscles could be applied to the deep shoulder girdle muscles by electroporation of different somitic levels, different parts of the somites and subsequent analysis of the derivatives (Masyuk et al. 2014; Morosan-Puopolo et al. 2014; Pu et al. 2013). In another study, Valasek and colleagues showed that a further group of secondary trunk muscles, the cloacal muscles, develops in a similar manner as the pectoral girdle muscles. First, these cells also migrate forward into the hindlimb and thereafter extend back toward the trunk. They describe this retrograde migration as an elongation of the ventral muscle mass of the hindlimb toward the cloaca (Valasek et al. 2005). Considering our live-cell imaging data, we assume a distinct mechanism for the retrograde migration of pectoral girdle muscle precursors. Proximal extension or elongation from a muscle mass inside the limb bud implies simultaneous migration of a coherent group of cells. In the present experimental setup, we could, however, observe individual cells actively migrating from the forelimb back toward the shoulder region. Yet further studies analyzing the gene expression pattern of pectoral girdle muscle precursors in the course of their migration are necessary in order to define the precise mode of pectoral girdle muscle development.

CXCR4/SDF-1 axis and development of pectoral girdle muscles

The wide-ranging involvement of the CXCR4/SDF-1 signaling in various migration processes led us to conjecture that this receptor-ligand system could be a molecular player in the formation of pectoral girdle muscles. We have previously reported the significance of these molecules during formation of another secondary trunk muscle group, the cloacal muscles in avians (Rehimi et al. 2010). In the present study, we unravel the role of CXCR4 and SDF-1 during formation of pectoral girdle muscles in two animal models, chicken and mice. In the context of forelimb muscle precursors, our and other groups have shown that the chemokine receptor CXCR4 is expressed by migrating myogenic precursors, while its ligand SDF-1 is secreted by the limb bud mesenchyme along the migration routes (Vasyutina et al. 2005; Yusuf and Brand-Saberi 2006). The expression patterns of CXCR4 and SDF-1 in chicken embryo have been previously described by our group (Yusuf et al. 2005; Rehimi et al. 2008). In the present study, we explicitly analyze the expression of CXCR4 and SDF-1 in the pectoral girdle region at the relevant stages and our results are highly suggestive for the role of this receptor-ligand pair in migrating myogenic precursor cells during development of pectoral girdle musculature. Furthermore, we already reported that molecular inhibitors of CXCR4 affect the migration of myogenic precursor cells into the limb bud (Yusuf and Brand-Saberi 2006). Here, we demonstrate that CXCR4 inhibitors affect the retrograde migration of myogenic precursors in chicken embryos, which is required for the formation of pectoral girdle muscles. The MyoD expression was reduced in the shoulder region after implantation of CXCR4-inhibitor-soaked beads. With the aid of live-cell imaging, we could provide evidence that this effect is due to a hindered retrograde migration of the myogenic precursors. The myogenic precursor cells moved actively, but did not succeed in penetrating

the CXCR4 inhibitor area, and thus, remained in the limb during the monitoring period. Indeed, one possible fate of these affected cells could be that they rest in the forelimb bud and undergo their differentiation program into muscle cells. There are indications for this as we could observe an apparent accumulation of MyoD-positive cells distal to the CXCR4 inhibitor bead. However, data of earlier studies argue against this hypothesis, as it was shown that progenitor cells, which were prevented from migration into the forelimb bud through CXCR4 inhibitors, underwent an altered differentiation program and developed into endothelial cells instead of muscle cells (Yusuf and Brand-Saberi 2006). Yet this issue has to be further investigated and quantified at the cellular level. Moreover, in our live-cell imaging data, we could observe that the myogenic precursors inhibited in their retrograde migration retained a high proliferation rate throughout the entire recording period. Thus, the CXCR4 inhibitor affects the active cell migration, but not a passive movement that may result from cell division. We thus conclude that the migration of the myogenic precursors back to the trunk occurs independently of cell proliferation.

To further support our studies in the chicken model, we show the importance of the CXCR4 signaling for the formation of the mammalian pectoral girdle musculature by additional use of a mouse model. In CXCR4−/− mouse embryos, we demonstrate a significant decrease of the muscle mass in specific pectoral girdle muscles as compared to the wildtype mouse embryo. Thus, we revealed the crucial role of CXCR4/SDF-1 axis for the pectoral girdle muscle formation also in mice. Remarkably, the pectoral girdle muscle blastemas in CXCR4-mutant mouse embryos are decreased but never absent, pointing toward a probable existence of $CXCR4^-$ subpopulations among the pectoral girdle muscle precursors. In the context of forelimb muscle precursors in mice, such a subdivision into $CXCR4^+$ and $CXCR4^-$ cells has been previously described (Vasyutina et al. 2005). Furthermore, we found in another study indications for a $CXCR4^-$ subpopulation during formation of cloacal muscles in chicken embryos (Rehimi et al. 2010). It is noteworthy that the formation of muscles of the distal forelimb bud is not affected in the CXCR4-mutant mouse embryos, as we could never observe a reduction of MyoD expression in this muscle group compared with the wildtype embryos. This is consistent with previous findings of Vasyutina and colleagues, who could not observe any appreciable changes in size of forelimb muscles in CXCR4-mutant mice. However, they found a pronounced reduction of forelimb muscle masses in CXCR4/Gab1 double-mutant mice, suggesting that CXCR4 signaling converges with signal transduction effectors used by Gab1 in mouse embryos (Vasyutina et al. 2005; Vasyutina and Birchmeier 2006).

Several cases of malformations of the pectoral girdle musculature in humans have been described (Hegde and Shokeir 1982; David and Winter 1985; Bergman et al. 1988; Paraskevas and Raikos 2010). The most common congenital disease affecting the shoulder girdle is Poland syndrome, with a prevalence of 1 in 20,000–30,000 live births. First described by Alfred Poland in 1841, it is characterized by unilateral absence or hypoplasia of pectoralis major and pectoralis minor muscle associated with ipsilateral skeletal, vascular and surface feature anomalies. Other clinical features occurring as part of Poland syndrome include malformations of the hand and narrowed sunken rib cage (Poland 1841; Jones 1926; Mosconi and Kamath 2003; Baban et al. 2009). The prevailing hypothesis concerning the etiology of Poland syndrome is a vascular perturbance during embryonic development affecting the subclavian artery (Bavinck and Weaver 1986). However, the pathogenesis of this disease remains completely unknown until today. Results from the present study suggest that interfering with the CXCR4/SDF-1 signaling in the shoulder region may account for defects reminiscent of human pectoral girdle malformations. Therefore, in addition to the vascular perturbance hypothesis, defects in migration pattern of myogenic precursors during embryogenesis have to be studied further. Investigation of the development of the pectoral girdle muscles can help to understand the underlying mechanisms of such congenital diseases as Poland syndrome and thus might be of clinical relevance in the future.

Conclusion

The present study demonstrates by live imaging the retrograde migration of myogenic precursor cells from the forelimb bud toward the trunk, visualized by in ovo electroporation and state-of-the-art confocal laser scanning microscopic time-lapse imaging. Hence, we verify the "In–Out" mechanism required for the formation of secondary trunk muscles of the pectoral girdle. Most importantly, we show that the retrograde migration of myogenic precursors is affected by blocking the CXCR4/SDF-1 axis in chicken embryos and provide evidence that the CXCR4/SDF-1 signaling is involved in the formation of pectoral girdle muscles in avians and mammals.

Acknowledgments The authors thank Prof. Dr. Ruijin Huang. M. Masyuk especially thanks FoRUM (RUB) for financial support by providing a dissertation scholarship. The authors further acknowledge S. Wulf, R. Houmany, and especially A. Lodwig for excellent technical assistance as well as A. Lenz and A. Conrad for secretarial work. This work was supported by MYORES project (511978) funded by the EU´s Sixth Framework Programme.

References

Baban A, Torre M, Bianca S, Buluggiu A, Rossello MI, Calevo MG, Valle M, Ravazzolo R, Jasonni V, Lerone M (2009) Poland syndrome with bilateral features: case description with review of the literature. Am J Med Genet A 149A(7):1597–1602

Balkwill F (2004) The significance of cancer cell expression of the chemokine receptor CXCR4. Semin Cancer Biol 14(3):171–179

Bavinck JN, Weaver DD (1986) Subclavian artery supply disruption sequence: hypothesis of a vascular etiology for Poland, Klippel-Feil, and Möbius anomalies. Am J Med Genet 23(4):903–918

Ben-Yair R, Kalcheim C (2005) Lineage analysis of the avian dermomyotome sheet reveals the existence of single cells with both dermal and muscle progenitor fates. Development 132(4):689–701

Ben-Yair R, Kalcheim C (2008) Notch and bone morphogenetic protein differentially act on dermomyotome cells to generate endothelium, smooth, and striated muscle. J Cell Biol 180(3):607–618

Ben-Yair R, Kahane N, Kalcheim C (2003) Coherent development of dermomyotome and dermis from the entire mediolateral extent of the dorsal somite. Development 130(18):4325–4336

Beresford B (1983) Brachial muscles in the chick embryo: the fate of individual somites. J Embryol Exp Morphol 77:99–116

Beresford B, Le Lievre C, Rathbone MP (1978) Chimaera studies of the origin and formation of the pectoral musculature of the avian embryo. J Exp Zool 205(2):321–326

Bergman RA, Thompson SA, Saadeh FA (1988) Anomalous fascicle and high origin of latissimus dorsi compensating for absence of serratus anterior. Anat Anz 167(2):161–164

Bladt F, Riethmacher D, Isenmann S, Aguzzi A, Birchmeier C (1995) Essential role for the c-met receptor in the migration of myogenic precursor cells into the limb bud. Nature 376(6543):768–771

Bleul CC, Fuhlbrigge RC, Casasnovas JM, Aiuti A, Springer TA (1996) A highly efficacious lymphocyte chemoattractant, stromal cell-derived factor 1 (SDF-1). J Exp Med 184(3):1101–1109

Bober E, Franz T, Arnold HH, Gruss P, Tremblay P (1994) Pax-3 is required for the development of limb muscles: a possible role for the migration of dermomyotomal muscle progenitor cells. Development 120(3):603–612

Brand-Saberi B, Wilting J, Ebensperger C, Christ B (1996) The formation of somite compartments in the avian embryo. Int J Dev Biol 40(1):411–420

Chevallier A, Kieny M, Mauger A (1977) Limb-somite relationship: origin of the limb musculature. J Embryol Exp Morphol 41:245–258

Christ B, Brand-Saberi B (2002) Limb muscle development. Int J Dev Biol 46(7):905–914

Christ B, Ordahl CP (1995) Early stages of chick somite development. Anat Embryol 191(5):381–396

Christ B, Jacob HJ, Jacob M (1977) Experimental analysis of the origin of the wing musculature in avian embryos. Anat Embryol 150(2):171–186

David TJ, Winter RM (1985) Familial absence of the pectoralis major, serratus anterior, and latissimus dorsi muscles. J Med Genet 22(5):390–392

Deng H, Liu R, Ellmeier W, Choe S, Unutmaz D, Burkhart M, Di Marzio P, Marmon S, Sutton RE, Hill CM, Davis CB, Peiper SC, Schall TJ, Littman DR, Landau NR (1996) Identification of a major co-receptor for primary isolates of HIV-1. Nature 381(6584):661–666

Dietrich S, Abou-Rebyeh F, Brohmann H, Bladt F, Sonnenberg-Riethmacher E, Yamaai T, Lumsden A, Brand-Saberi B, Birchmeier C (1999) The role of SF/HGF and c-Met in the development of skeletal muscle. Development 126(8):1621–1629

Doitsidou M, Reichman-Fried M, Stebler J, Köprunner M, Dörries J, Meyer D, Esguerra CV, Leung T, Raz E (2002) Guidance of primordial germ cell migration by the chemokine SDF-1. Cell 111(5):647–659

Doranz BJ, Rucker J, Yi Y, Smyth RJ, Samson M, Peiper SC, Parmentier M, Collman RG, Doms RW (1996) A dual-tropic primary HIV-1 isolate that uses fusin and the beta-chemokine receptors CKR-5, CKR-3, and CKR-2b as fusion cofactors. Cell 85(7):1149–1158

Feng Y, Broder CC, Kennedy PE, Berger EA (1996) HIV-1 entry cofactor: functional cDNA cloning of a seven-transmembrane, G protein-coupled receptor. Science 272(5263):872–877

Franz T, Kothary R, Surani MA, Halata Z, Grim M (1993) The Splotch mutation interferes with muscle development in the limbs. Anat Embryol 187(2):153–160

Gavrieli Y, Sherman Y, Ben-Sasson SA (1992) Identification of programmed cell death in situ via specific labeling of nuclear DNA fragmentation. J Cell Biol 119(3):493–501

Grim M (1971) Development of the primordia of the latissimus dorsi muscle of the chicken. Folia Morphol 19(3):252–258

Hamburger V, Hamilton HL (1951) A series of normal stages in the development of the chick embryo. J Morphol 88:1

Hegde HR, Shokeir MH (1982) Posterior shoulder girdle abnormalities with absence of pectoralis major muscle. Am J Med Genet 13(3):285–293

Hiratsuka S, Duda DG, Huang Y, Goel S, Sugiyama T, Nagasawa T, Fukumura D, Jain RK (2011) C-X-C receptor type 4 promotes metastasis by activating p38 mitogen-activated protein kinase in myeloid differentiation antigen (Gr-1)-positive cells. Proc Natl Acad Sci USA 108(1):302–307

Huang R, Christ B (2000) Origin of the epaxial and hypaxial myotome in avian embryos. Anat Embryol 202(5):369–374

Jones HW (1926) Congenital absence of the pectoral muscles. Br Med J 6:59–60

Kalcheim C, Cinnamon Y, Kahane N (1999) Myotome formation: a multistage process. Cell Tissue Res 296(1):161–173

Kawakami K (2007) Tol2: a versatile gene transfer vector in vertebrates. Genome Biol 8(Suppl 1):S7

Kawakami K, Shima A, Kawakami N (2000) Identification of a functional transposase of the Tol2 element, an Ac-like element from the Japanese medaka fish, and its transposition in the zebrafish germ lineage. Proc Natl Acad Sci USA 97(21):11403–11408

Knaut H, Werz C, Geisler R, Nüsslein-Volhard C, Tübingen 2000 Screen Consortium (2003) A zebrafish homologue of the chemokine receptor Cxcr4 is a germ-cell guidance receptor. Nature 421(6920):279–282

Koga A, Suzuki M, Inagaki H, Bessho Y, Hori H (1996) Transposable element in fish. Nature 383(6595):30

Krull CE (2004) A primer on using in ovo electroporation to analyze gene function. Dev Dyn 229(3):433–439

Lanser ME, Fallon JF (1987) Development of wing-bud-derived muscles in normal and wingless chick embryos: a computer-assisted three-dimensional reconstruction study of muscle pattern formation in the absence of skeletal elements. Anat Rec 217(1):61–78

Lazarini F, Tham TN, Casanova P, Arenzana-Seisdedos F, Dubois-Dalcq M (2003) Role of the alpha-chemokine stromal cell-derived factor (SDF-1) in the developing and mature central nervous system. Glia 42(2):139–148

Ma Q, Jones D, Borghesani PR, Segal RA, Nagasawa T, Kishimoto T, Bronson RT, Springer TA (1998) Impaired B-lymphopoiesis, myelopoiesis, and derailed cerebellar neuron migration in CXCR4- and SDF-1-deficient mice. Proc Natl Acad Sci USA 95(16):9448–9453

Mansouri A, Hallonet M, Gruss P (1996) Pax genes and their roles in cell differentiation and development. Curr Opin Cell Biol 8(6):851–857

Marcelle C, Wolf J, Bronner-Fraser M (1995) The in vivo expression of the FGF receptor FREK mRNA in avian myoblasts

suggests a role in muscle growth and differentiation. Dev Biol 172(1):100–114
Masyuk M, Morosan-Puopolo G, Brand-Saberi B, Theiss C (2014) Combination of in ovo electroporation and time-lapse imaging to study migrational events in chicken embryos. Dev Dyn 243(5):690–698
Mauger A (1972a) The role of somitic mesoderm in the development of dorsal plumage in chick embryos. I. Origin, regulative capacity and determination of the plumage-forming mesoderm. J Embryol Exp Morphol 28(2):313–341 (article in French)
Mauger A (1972b) The role of somitic mesoderm in the development of dorsal plumage in chick embryos. II. Regionalization of the plumage-forming mesoderm. J Embryol Exp Morphol 28(2):343–366 (article in French)
Morosan-Puopolo G, Balakrishnan-Renuka A, Yusuf F, Chen J, Dai F, Zoidl G, Lüdtke TH, Kispert A, Theiss C, Abdelsabour-Khalaf M, Brand-Saberi B (2014) Wnt11 is required for oriented migration of dermogenic progenitor cells from the dorsomedial lip of the avian dermomyotome. PLoS ONE 9(3):e92679
Mosconi T, Kamath S (2003) Bilateral asymmetric deficiency of the pectoralis major muscle. Clin Anat 16(4):346–349
Müller A, Homey B, Soto H, Ge N, Catron D, Buchanan ME, McClanahan T, Murphy E, Yuan W, Wagner SN, Barrera JL, Mohar A, Verástegui E, Zlotnik A (2001) Involvement of chemokine receptors in breast cancer metastasis. Nature 410(6824):50–56
Nagashima H, Sugahara F, Takechi M, Ericsson R, Kawashima-Ohya Y, Narita Y, Kuratani S (2009) Evolution of the turtle body plan by the folding and creation of new muscle connections. Science 325(5937):193–196
Nieto MA, Patel K, Wilkinson DG (1996) In situ hybridization analysis of chick embryos in whole mount and tissue sections. Methods Cell Biol 51:219–235
Olivera-Martinez I, Coltey M, Dhouailly D, Pourquié O (2000) Mediolateral somitic origin of ribs and dermis determined by quail-chick chimeras. Development 127(21):4611–4617
Olivera-Martinez I, Missier S, Fraboulet S, Thélu J, Dhouailly D (2002) Differential regulation of the chick dorsal thoracic dermal progenitors from the medial dermomyotome. Development 129(20):4763–4772
Olivera-Martinez I, Thélu J, Dhouailly D (2004) Molecular mechanisms controlling dorsal dermis generation from the somitic dermomyotome. Int J Dev Biol 48(2–3):93–101
Ordahl CP, Le Douarin NM (1992) Two myogenic lineages within the developing somite. Development 114(2):339–353
Ott MO, Bober E, Lyons G, Arnold H, Buckingham M (1991) Early expression of the myogenic regulatory gene, myf-5, in precursor cells of skeletal muscle in the mouse embryo. Development 111(4):1097–1107
Paraskevas GK, Raikos A (2010) Bilateral pectoral musculature malformations with concomitant vascular anomaly. Folia Morphol 69(3):187–191
Poland A (1841) Deficiency of the pectoral muscles. Guys Hosp Rep 6:191–193
Pownall ME, Emerson CP Jr (1992) Sequential activation of three myogenic regulatory genes during somite morphogenesis in quail embryos. Dev Biol 151(1):67–79
Pu Q, Abduelmula A, Masyuk M, Theiss C, Schwandulla D, Hans M, Patel K, Brand-Saberi B, Huang R (2013) The dermomyotome ventrolateral lip is essential for the hypaxial myotome formation. BMC Dev Biol 13:37
Pujol F, Kitabgi P, Boudin H (2005) The chemokine SDF-1 differentially regulates axonal elongation and branching in hippocampal neurons. J Cell Sci 118(Pt 5):1071–1080
Rehimi R, Khalida N, Yusuf F, Dai F, Morosan-Puopolo G, Brand-Saberi B (2008) Stromal-derived factor-1 (SDF-1) expression during early chick development. Int J Dev Biol 52(1):87–92
Rehimi R, Khalida N, Yusuf F, Morosan-Puopolo G, Brand-Saberi B (2010) A novel role of CXCR4 and SDF-1 during migration of cloacal muscle precursors. Dev Dyn 239(6):1622–1631
Sassoon DA (1993) Myogenic regulatory factors: dissecting their role and regulation during vertebrate embryogenesis. Dev Biol 156(1):11–23
Sato Y, Kasai T, Nakagawa S, Tanabe K, Watanabe T, Kawakami K, Takahashi Y (2007) Stable integration and conditional expression of electroporated transgenes in chicken embryos. Dev Biol 305(2):616–624
Stebler J, Spieler D, Slanchev K, Molyneaux KA, Richter U, Cojocaru V, Tarabykin V, Wylie C, Kessel M, Raz E (2004) Primordial germ cell migration in the chick and mouse embryo: the role of the chemokine SDF-1/CXCL12. Dev Biol 272(2):351–361
Sullivan GE (1962) Anatomy and embryology of the wing musculature of the domestic fowl (Gallus). Aust J Zool 10:458–516
Tajbakhsh S, Rocancourt D, Cossu G, Buckingham M (1997) Redefining the genetic hierarchies controlling skeletal myogenesis: Pax-3 and Myf-5 act upstream of MyoD. Cell 89(1):127–138
Tamamura H, Xu Y, Hattori T, Zhang X, Arakaki R, Kanbara K, Omagari A, Otaka A, Ibuka T, Yamamoto N, Nakashima H, Fujii N (1998) A low-molecular-weight inhibitor against the chemokine receptor CXCR4: a strong anti-HIV peptide T140. Biochem Biophys Res Commun 253(3):877–882
Tamamura H, Omagari A, Hiramatsu K, Gotoh K, Kanamoto T, Xu Y, Kodama E, Matsuoka M, Hattori T, Yamamoto N, Nakashima H, Otaka A, Fujii N (2001) Development of specific CXCR4 inhibitors possessing high selectivity indexes as well as complete stability in serum based on an anti-HIV peptide T140. Bioorg Med Chem Lett 11(14):1897–1902
Valasek P, Evans DJ, Maina F, Grim M, Patel K (2005) A dual fate of the hindlimb muscle mass: cloacal/perineal musculature develops from leg muscle cells. Development 132(3):447–458
Valasek P, Theis S, DeLaurier A, Hinits Y, Luke GN, Otto AM, Minchin J, He L, Christ B, Brooks G, Sang H, Evans DJ, Logan M, Huang R, Patel K (2011) Cellular and molecular investigations into the development of the pectoral girdle. Dev Biol 357(1):108–116
Vasyutina E, Birchmeier C (2006) The development of migrating muscle precursor cells. Anat Embryol 211(Suppl 1):37–41
Vasyutina E, Stebler J, Brand-Saberi B, Schulz S, Raz E, Birchmeier C (2005) CXCR4 and Gab1 cooperate to control the development of migrating muscle progenitor cells. Genes Dev 19(18):2187–2198
Wilting J, Brand-Saberi B, Huang R, Zhi Q, Köntges G, Ordahl CP, Christ B (1995) Angiogenic potential of the avian somite. Dev Dyn 202(2):165–171
Wilting J, Schneider M, Papoutski M, Alitalo K, Christ B (2000) An avian model for studies of embryonic lymphangiogenesis. Lymphology 33(3):81–94
Wilting J, Papoutsi M, Othman-Hassan K, Rodriguez-Niedenführ M, Pröls F, Tomarev SI, Eichmann A (2001) Development of the avian lymphatic system. Microsc Res Tech 55(2):81–91
Yusuf F, Brand-Saberi B (2006) The eventful somite: patterning, fate determination and cell division in the somite. Anat Embryol 211(Suppl 1):21–30
Yusuf F, Brand-Saberi B (2012) Myogenesis and muscle regeneration. Histochem Cell Biol 138(2):187–199
Yusuf F, Rehimi R, Dai F, Brand-Saberi B (2005) Expression of chemokine receptor CXCR4 during chick embryo development. Anat Embryol 210(1):35–41
Zou YR, Kottmann AH, Kuroda M, Taniuchi I, Littman DR (1998) Function of the chemokine receptor CXCR4 in haematopoiesis and in cerebellar development. Nature 393(6685):595–599

Tetrahedron 70 (2014) 5122–5127

Contents lists available at ScienceDirect

Tetrahedron

journal homepage: www.elsevier.com/locate/tet

Development of a fluoride-responsive amide bond cleavage device that is potentially applicable to a traceable linker

Jun Yamamoto [a,†], Nami Maeda [a,†], Chiaki Komiya [a], Tomohiro Tanaka [b], Masaya Denda [a], Koji Ebisuno [a], Wataru Nomura [b], Hirokazu Tamamura [b], Youichi Sato [c], Aiko Yamauchi [c], Akira Shigenaga [a,d,*], Akira Otaka [a,*]

[a] Department of Bioorganic Synthetic Chemistry, Institute of Health Biosciences and Graduate School of Pharmaceutical Sciences, The University of Tokushima, Shomachi, Tokushima 770-8505, Japan
[b] Institute of Biomaterials and Bioengineering, Tokyo Medical and Dental University, Chiyoda-ku, Tokyo 101-0062, Japan
[c] Department of Pharmaceutical Information Science, Institute of Health Biosciences and Graduate School of Pharmaceutical Sciences, The University of Tokushima, Shomachi, Tokushima 770-8505, Japan
[d] JST, PRESTO, 4-1-8 Honcho, Kawaguchi, Saitama 332-0012, Japan

ARTICLE INFO

Article history:
Received 28 April 2014
Received in revised form 29 May 2014
Accepted 31 May 2014
Available online 6 June 2014

Keywords:
Cleavable linker
Fluoride-responsive
Traceable linker
Stimulus-responsive amino acid

ABSTRACT

A fluoride-responsive (FR) amino acid that induces amide bond cleavage upon the addition of a fluoride was developed, and it was applied to an FR traceable linker. By the use of an alkyne-containing peptide as a model of an alkynylated target protein of a bioactive compound, introduction of the FR traceable linker onto the peptide was achieved. Subsequent fluoride-induced cleavage of the linker followed by labeling of the released peptide derivative was also conducted to examine the potential applicability of the FR traceable linker to the enrichment and labeling of alkynylated target molecules.

1. Introduction

A wide variety of molecules including natural products, peptides, and synthetic small compounds exhibit their biological activities through specific interactions with target biomacromolecules. Proteins including enzymes, receptors, and ion channels represent the major group of these targets. Identification of unknown protein targets that interact with biologically active ligands has become indispensable in the fields of chemical biology and drug development; however, this research approach is time-consuming and laborious. The target identification comprises a sequence of processes: (1) fishing a target using a biologically active ligand as bait; (2) enrichment of the hooked target; and (3) sequence analysis of the target by Edman degradation or mass spectrometry (MS).[1] For the first step, photo-affinity labeling, which allows bait to be covalently bounded to the corresponding target upon photo-irradiation has significant use, because of the potential applicability to low affinity ligand-target pairs.[1a,b,2] The hooked target is then linked with a biotinylated linker molecule for facile purification by streptavidin beads using the biotin–streptavidin interaction.[1,3] The immobilized target is subsequently released from the beads for sequence analysis by attenuating the biotin–streptavidin interaction. The high affinity of the biotin–streptavidin interaction (K_d=10^{-15} M),[4] however, hampers liberation of the target from the beads. An alternative to liberate the target is the use of a cleavable linker between the bait and biotin.[5] This approach enables efficient elution of the target protein from the beads via the linker cleavage, but contamination owing to the presence of non-target proteins sometimes hampers identification of the target.[6] The cleavage under mild conditions and generation of an orthogonal functional group not seen in proteins, therefore, has been desired in this procedure. The orthogonal functional group enables chemoselective labeling of the target protein by an isotopic or fluorescent tag. That facilitates discrimination of the target from contaminated proteins by MS using isotopic tag or SDS-PAGE using fluorescent tag.

We previously developed a traceable linker as an advanced cleavable linker that enables selective labeling of the target protein after elution from the streptavidin beads via the linker cleavage

* Corresponding authors. Tel.: +81 88 633 9534; fax: +81 88 633 9505; e-mail addresses: shigenaga.akira@tokushima-u.ac.jp (A. Shigenaga), aotaka@tokushima-u.ac.jp (A. Otaka).
† These authors contributed equally to this work.

http://dx.doi.org/10.1016/j.tet.2014.05.110
0040-4020/